



The Abdus Salam
International Centre for Theoretical Physics



SMR.1670 - 36

INTRODUCTION TO MICROFLUIDICS

8 - 26 August 2005

Fluid Mechanics Theory

S. Wereley
Purdue University, U.S.A.

ICTP Microfluidics 2005

Prof. Steve Wereley
Purdue University
Mechanical Engineering
wereley@purdue.edu
www.ecn.purdue.edu/microfluidics



Wereley Lectures Overview (first couple)

1. Introductions
2. Fluid mechanics theory
 - a. Small but continuous flows
 - b. Sub-continuum flows
3. Surface tension
4. Electrokinetics
5. Microdomain practicalities
6. Characterization of microflows



1. Introductions

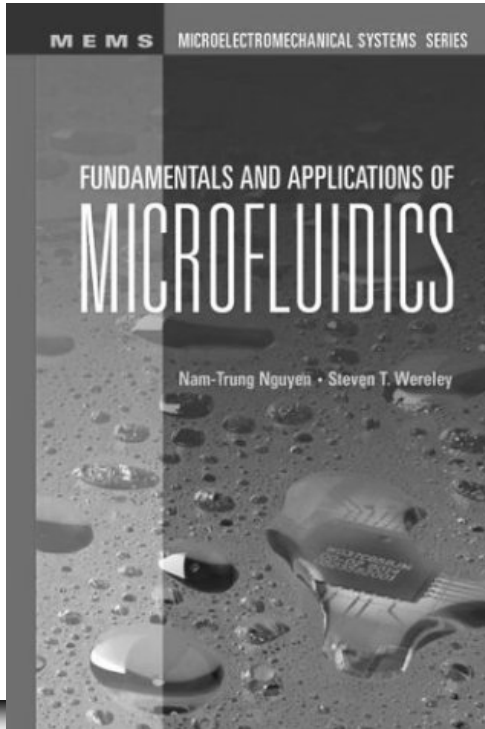


About your instructor...

- Steve Wereley
 - Mechanical Engineering, Purdue University
 - 7 years' experience in micro/nano flows
 - Co-author of *Fundamentals and Applications of Microfluidics* (with N.T. Nguyen)
 - Patented and licensed microfluidic measurement technique *micro-PIV*
 - Active in many different areas of micro/nano fluid dynamics
 - Rarefied gas dynamics
 - Micro flows
 - Subcontinuum (i.e. nano) flows
 - BioMEMS



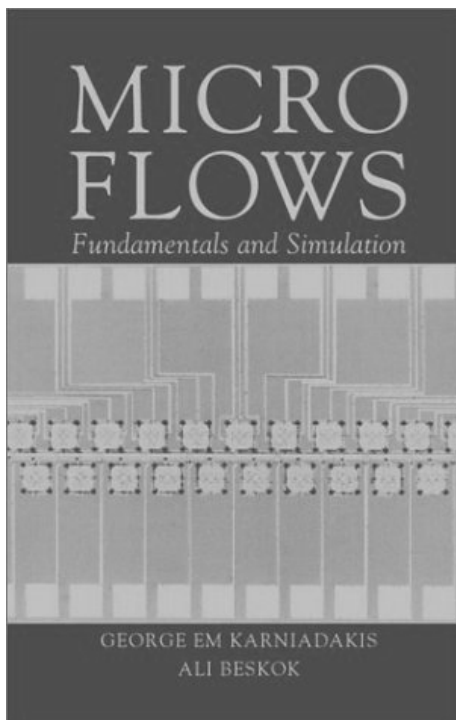
A bit of a commercial...



- Microfluidics textbook
- Published 2002
- Available from **artechhouse.com** or **amazon.com**
- Micro/nano flow phenomena explored using practical examples
- Source for any unattributed material in this presentation



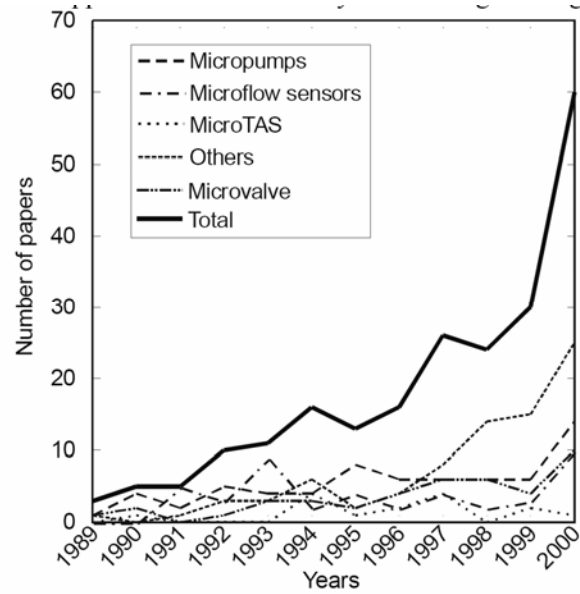
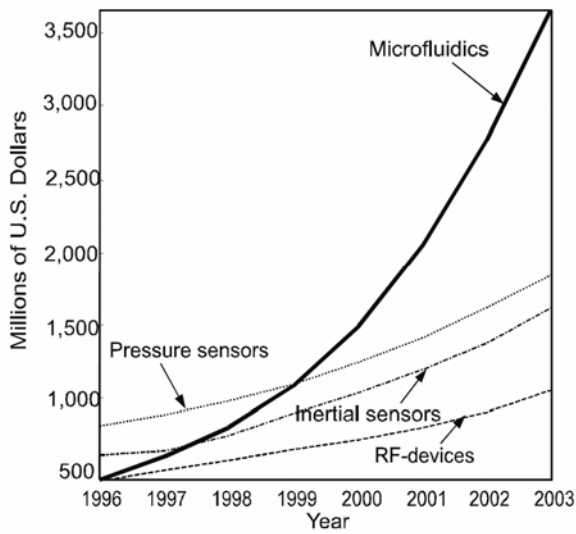
Some representation for the competition...



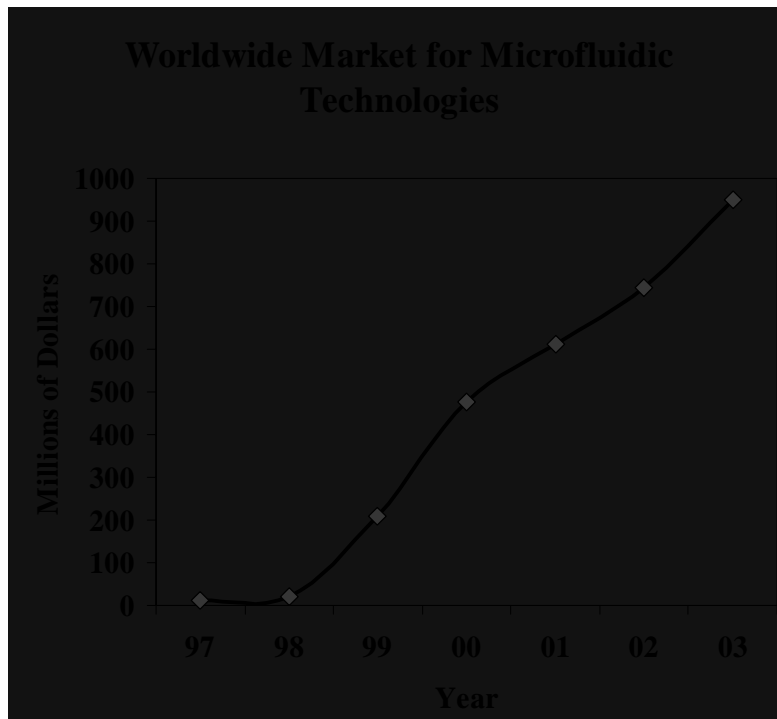
- Recent title from Springer (2001)
- Second edition due out soon
- Very good book if your interest is simulations
 - DSMC
 - Boltzmann



Commercial/Academic Interest



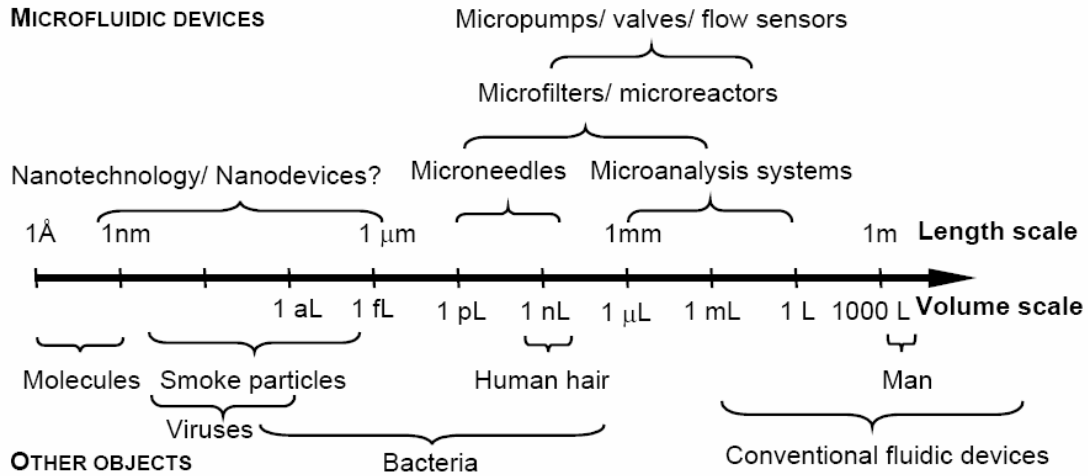
These kinds of figures are from Nguyen and Wereley



- According to *Business Communications Co., Inc.*
- Expected annual growth rate through 2008: **15.5%**

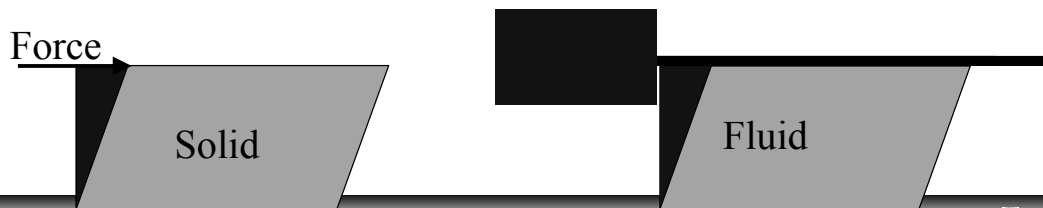


Microfluidics Length Scales/Applications



Fluid Fundamentals

- **Definition:**
A fluid is a substance that deforms continuously under the application of a shear (tangential) stress no matter how small the shear stress may be.
- Liquids and gases are very different animals
 - Liquids become *less* viscous as T increases
 - Gases become *more* viscous at T increases



Fundamental Macro Assumptions

- Fluid behaves as a continuum
- Fluid 'sticks' to surfaces (no-slip condition)
- Fairly high Reynolds number (Re)
 $Re = \text{inertial forces} / \text{viscous forces}$
implies inertia relatively important



2. Fluid Mechanics at Microscopic Length Scales

1. Behavioral Changes at Small Length Scales
2. Length Scales at Which Behavioral Changes Become Important
3. Fluid modeling
 1. Continuum model
 2. Molecular-based models
4. Boundary conditions

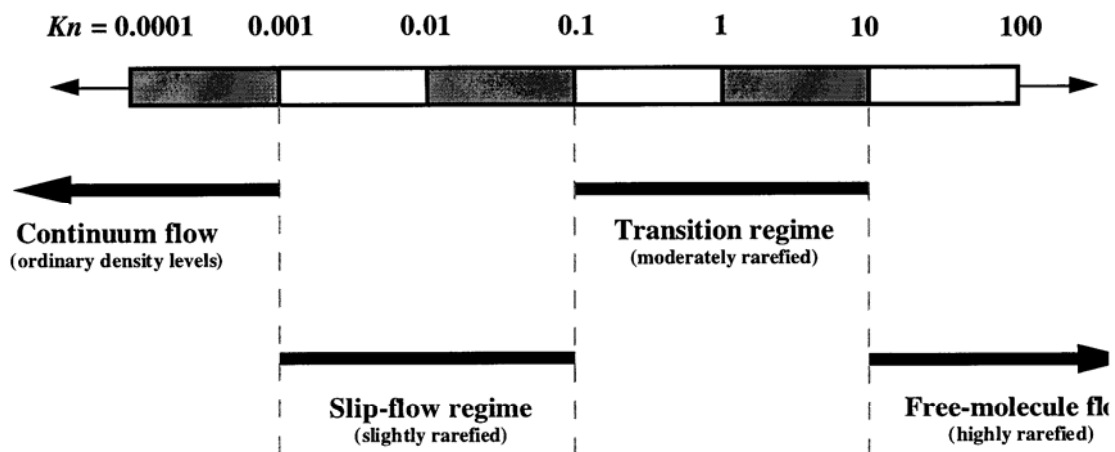


Reasons for Fluid Behavioral Changes

- Cube-Square Law
 - quantities $\propto L^3$
 - inertia, buoyancy, etc.
 - quantities $\propto L^2$
 - drag, surface charge, etc.
 - quantities $\propto L^1$
 - surface tension
- Non-continuum effects
 - gases: $Kn = \lambda/L$, no slip, continuum approximation
 - liquids: complex behaviors as continuum assumption breaks down



Knudsen Number Regimes (*only for gases*)

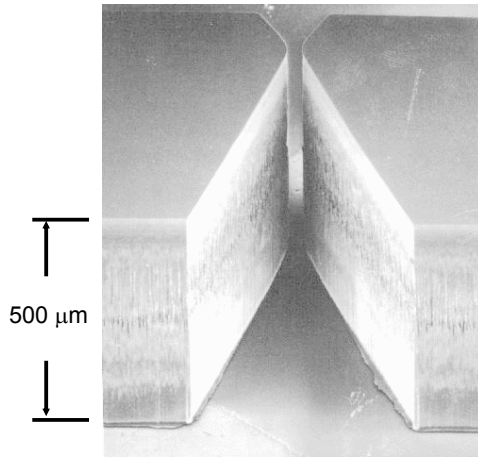


Knudsen number regimes.

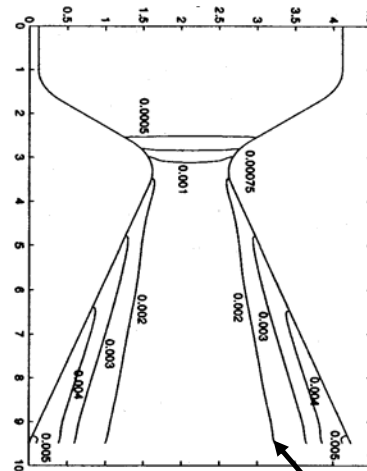
Gad-el-Hak, 1999



MEMS-based Supersonic Microthruster Example



(End View)



(Top View)

contours
of Kn

$$Kn = \sqrt{\frac{\pi\gamma}{2}} \cdot \frac{M}{Re}$$

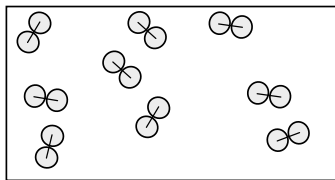
(Courtesy: Bayt and Breuer, MIT)

γ is gas prop ratio of specific heats ~ 1.4

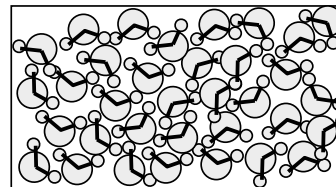


The Smallest Length Scale of a Continuum (Deen, Analysis of Transport Phenomena, 1998)

Gases (STP)



Liquids



Molecular diameter 0.3 nm
 Number density (m^{-3}) 3 E25
 Intermolecular spacing 3 nm
 Displacement distance 100 nm
 Molecular Velocity 500 m/s

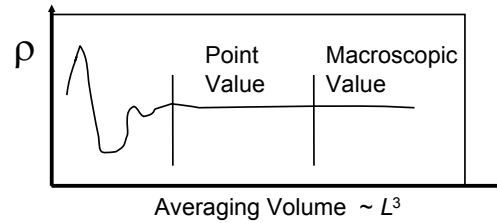
Molecular diameter 0.3 nm
 Number density (m^{-3}) 2 E28
 Intermolecular spacing 0.4 nm
 Displacement distance 1 pm
 Molecular Velocity 10^3 m/s



The Smallest Length Scale of a Continuum (Deen, Analysis of Transport Phenomena, 1998)

Average over sufficient number of molecules

- Point quantities, ρ , \mathbf{u} , T



- Random process theory
 - $N \sim 10^4$ molecules $\sigma_\mu = \frac{\sigma_x}{N^{1/2}}$
- $L \sim 70$ nm (gases at STP)
- $L \sim 8$ nm (liquids)



The Smallest Length Scale of a Continuum (Deen, Analysis of Transport Phenomena, 1998)

Length scale of molecular interactions
(transport properties, μ , κ , D)

- Gases: mean free path ~ 100 nm
- Liquids: molecular diameter ~ 0.3 nm

Average over $\sim 10^3$ interaction length scales

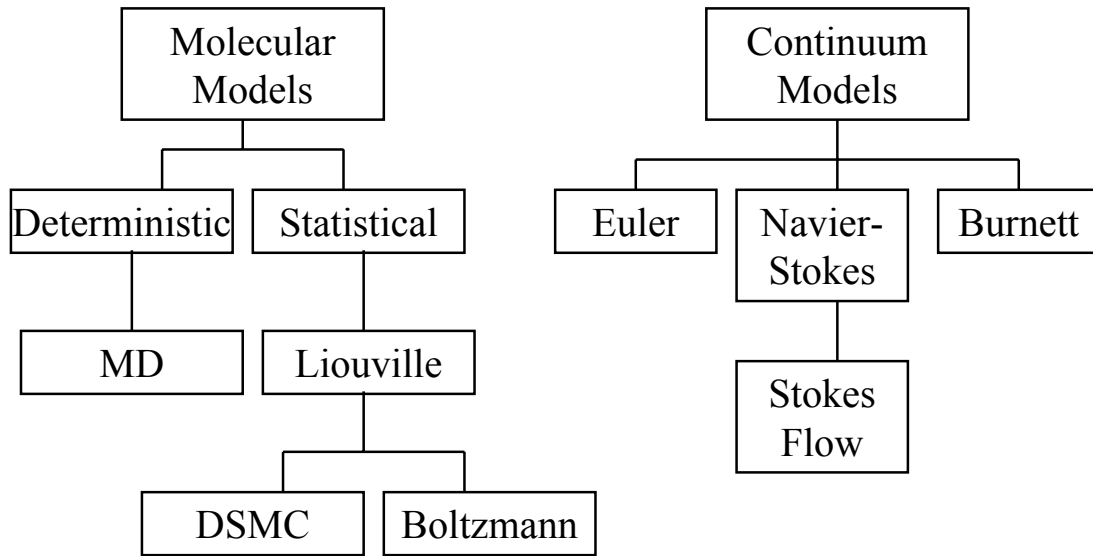
- $L \sim 1$ μm (gases)
- $L \sim 3$ nm (liquids)

Taking the max of these two quantities

- $L_{cont} \sim 1$ μm (gases)
- $L_{cont} \sim 10$ nm (liquids)



Fluid Modeling Family Tree



Continuum Models



Navier Stokes Equation (dimensional form)

$$\rho \frac{D\vec{V}}{Dt} = \rho \frac{\partial \vec{V}}{\partial t} + \rho (\vec{V} \cdot \nabla) \vec{V} = -\nabla p + \mu \nabla^2 \vec{V}$$

$$\vec{V} = u \vec{V}'$$

$$\vec{x} = L \vec{x}'$$

$$p = \frac{\mu u}{L} p'$$

$$t = \frac{L}{u} t'$$

where u is characteristic velocity such as mean velocity, centerline velocity, etc., L is characteristic size of system such as pipe diameter, local BL thickness

From these quantities construct scales for time and pressure



Navier-Stokes Equation (Dimensionless)

$$\text{Re} \frac{D\vec{V}}{Dt} = \text{Re} \left(\frac{\partial \vec{V}}{\partial t} + (\vec{V} \cdot \nabla) \vec{V} \right) = -\nabla p + \nabla^2 \vec{V}$$

$$\text{where } \text{Re} = \frac{\rho u L}{\mu}$$

- Re=Reynolds number, ratio of inertial forces to viscous forces
- All variables normalized so that they are order unity



Stokes Flows

- Assume we're considering a water flow
 - $\mu=10^{-3}$ kg/(s m), $\rho=10^3$ kg/m³
- Length scale: $10\ \mu\text{m}=10^{-5}$ m
- Velocity scale: $10\ \text{mm/s}=10^{-2}$ m/s
- Then: $\text{Re}=10^{-1}$, so N-S eqn

$$0 = -\nabla p + \nabla^2 \vec{V}$$

- becomes Poisson Eqn (Stokes Flow), simple, linear equation



Boundary Conditions

Generalized slip flow model for *liquid or gas*:

$$\Delta u|_{\text{wall}} = u_{\text{fluid}} - u_{\text{wall}} = L_s \left. \frac{\partial u}{\partial y} \right|_{\text{wall}}$$

Slip flow model *strictly for ideal gases*:

$$u_{\text{gas}} - u_{\text{wall}} = \lambda \left. \frac{2 - \sigma_v}{\sigma_v} \frac{\partial u}{\partial y} \right|_{\text{wall}} + \frac{3}{4} \frac{\mu}{\rho T_{\text{gas}}} \left. \frac{\partial T}{\partial x} \right|_{\text{wall}}$$

Dimensionless Slip flow model for ideal gas:

$$u_{\text{gas}}^* - u_{\text{wall}}^* = Kn \left. \frac{2 - \sigma_v}{\sigma_v} \frac{\partial u^*}{\partial y^*} \right|_{\text{wall}} + \frac{3}{2\pi} \frac{\gamma - 1}{\gamma} \frac{Kn^2 \text{Re}}{Ec} \left. \frac{\partial T^*}{\partial x^*} \right|_{\text{wall}}$$



Gas Accommodation Coefficients

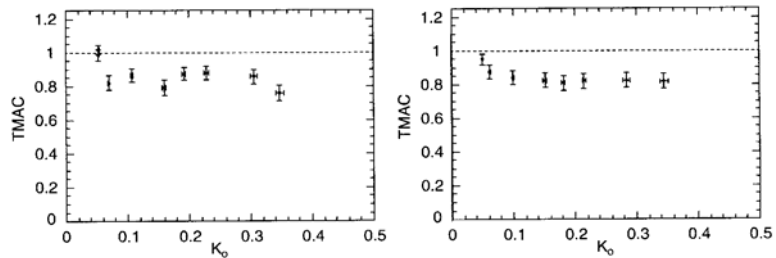
Accommodation coefficients are macro/molecular quantities that depend on

- gas type
- surface material
- surface topology

Gas	Metal	σ_v	σ_T
Air	Aluminum	0.87-0.97	0.87-0.97
Air	Iron	0.87-0.96	0.87-0.93
Air	Bronze	0.88-0.95	n/a
Ar	Silicon	0.80-0.90	n/a
N ₂	Silicon	0.80-0.85	n/a

$$\sigma_v = \frac{\tau_i - \tau_r}{\tau_i - \tau_w}$$

$$\sigma_T = \frac{dE_i - dE_r}{dE_i - dE_w}$$

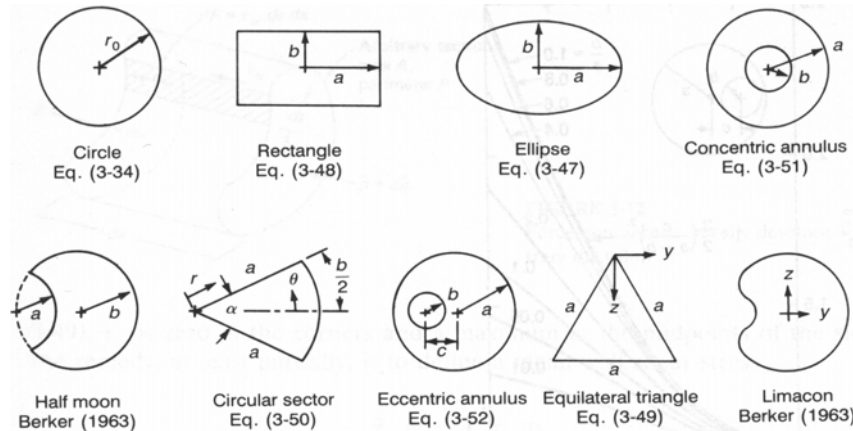


Beskok, 2002

FIGURE 2.3. Tangential momentum accommodation coefficient σ_v (TMAC) versus Knudsen number obtained from mass flowrate measurements for argon (left) and for nitrogen (right) (see details in (Arkilic, 1997)). (Courtesy of K. Breuer)



Continuum incompressible flow through long channels (White, 1991)



$$u = \frac{-d\hat{p}/dx}{4\mu} (r_0^2 - r^2)$$

$$Q_{\text{pipe}} = \frac{\pi r_0^4}{8\mu} \left(-\frac{d\hat{p}}{dx} \right)$$

$$u(y, z) = \frac{16a^2}{\mu\pi^3} \left(-\frac{d\hat{p}}{dx} \right) \sum_{i=1,3,5,\dots}^{\infty} (-1)^{(i-1)/2} \left[1 - \frac{\cosh(i\pi z/2a)}{\cosh(i\pi b/2a)} \right] \times \frac{\cos(i\pi y/2a)}{i^3}$$

$$u(y, z) = \frac{-d\hat{p}/dx}{2\sqrt{3}a\mu} \left(z - \frac{1}{2}a\sqrt{3} \right) (3y^2 - z^2)$$

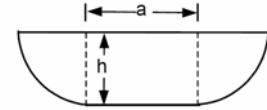
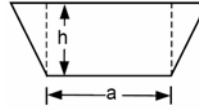
$$Q = \frac{4ba^3}{3\mu} \left(-\frac{d\hat{p}}{dx} \right) \left[1 - \frac{192a}{\pi^5 b} \sum_{i=1,3,5,\dots}^{\infty} \frac{\tanh(i\pi b/2a)}{i^5} \right]$$

$$Q = \frac{a^4\sqrt{3}}{320\mu} \left(-\frac{d\hat{p}}{dx} \right)$$



Shapes *NOT* represented in table

- Two additional useful shapes:
 - Trapezoid
 - Rectangle with two rounded corners
 - I have not found any references that provide these solutions—should be easy paper in microfluidics
- For shapes in which we don't have analytical solution
 - Approximate approach
 - Hydraulic diameter ($4 \cdot \text{Area} / \text{Perimeter}$)
 - Plug into circle expression for Q versus ΔP



Molecular Models



Molecular Interaction Forces: Lennard-Jones 6-12 Potential

$$V_{ij}(r) = 4\epsilon \left[c_{ij} \left(\frac{r}{\sigma} \right)^{-12} - d_{ij} \left(\frac{r}{\sigma} \right)^{-6} \right] \quad F_{ij}(r) = -\frac{\partial V_{ij}}{\partial r} = \frac{48\epsilon}{\sigma} \left[c_{ij} \left(\frac{r}{\sigma} \right)^{-13} - \frac{d_{ij}}{2} \left(\frac{r}{\sigma} \right)^{-7} \right]$$

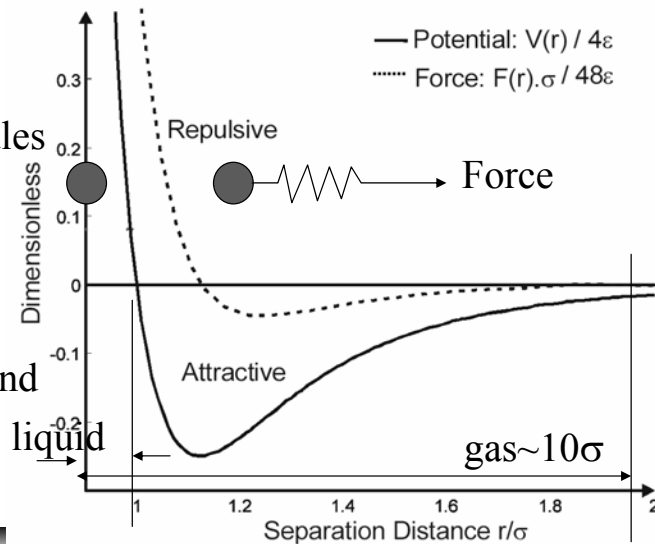
V_{ij} = potential energy between two molecules i and j

F_{ij} = force between two molecules i and j

c_{ij} and d_{ij} are parameters for chosen molecules

ϵ, σ are characteristic energy and length scales respectively

r is the separation distance



Lennard Jones Constants

Fluid	ϵ/K (K)	σ (nm)
Air	97	0.362
N ₂	91.5	0.368
CO ₂	190	0.400
O ₂	113	0.343
Ar	124	0.342

Phases	Intermolecular Forces	Ratio of Thermal Vibration Amplitude Compared to σ	Approach Needed
Solid	Strong	$\ll 1$	Quantum
Liquid	Moderate	~ 1	Quantum/classical
Gas	Weak	$\gg 1$	Classical



Molecular Dynamics Governing Equations

$$m \frac{d^2 \mathbf{r}_i}{dt^2} = \sum_{j \neq i} \frac{\partial V_{ij}}{\partial \mathbf{r}_i} - \frac{m}{\tau} \frac{d\mathbf{r}_i}{dt} + \eta_i \quad \tau = \sqrt{\frac{\sigma^2 m}{\varepsilon}}$$

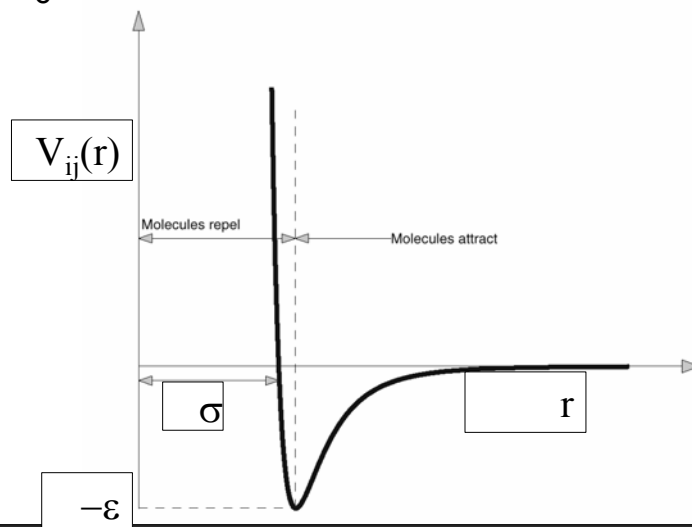
- where \mathbf{r}_i is the position vector, V_{ij} is the potential energy between any two molecules, τ is characteristic time scale, m is atomic mass
- Last two terms on RHS couple the particle dynamics with thermodynamics
 - Velocity term governs heat exchange with reservoir
 - η_i term is a Gaussian stochastic force with variance $2mk_b/\tau$
- For liquid argon, $\tau=2.2^{-12}$ sec
- Evolve the position of every molecule forward in time using Newton's 2nd Law



Shifted Lennard-Jones Potential

$$V_{ij}(r) = 4\varepsilon \left[c_{ij} \left(\frac{r}{\sigma} \right)^{-12} - d_{ij} \left(\frac{r}{\sigma} \right)^{-6} - \left(c_{ij} \left(\frac{r_c}{\sigma} \right)^{-12} - d_{ij} \left(\frac{r_c}{\sigma} \right)^{-6} \right) \right]$$

- r_c is cut-off radius, typically $2.2\sigma < r_c < 2.5\sigma$



Lennard-Jones Potential

- Works reasonably well for electrically neutral, polarizable, spherical molecules
- Dynamics for immiscible liquids ($d_{12}=d_{21}$)
 - $d_{12}=0$ implies pure short-range repulsion
 - $d_{12}=1$ implies symmetric interaction
 - $d_{12}>$ implies enhanced attraction
- Dynamics of wall boundaries can be simulated with same L-J approach but different constants
- Complicated molecules require complicated potentials, e.g. polymer chains can have a potential between all monomers plus a strongly attractive potential when all monomers in neighboring molecules line up



Temporal Evolution

- Equations of motions can be integrated forward in time by typical predictor-corrector scheme
 - typical time step size $\Delta t=0.005\tau$
 - for liquid Ar, $\Delta t=1.1e-14$ sec
- Another commonly used discretization called Verlet integration rule is

$$\mathbf{r}^{n+1} = 2\mathbf{r}^n - \mathbf{r}^{n-1} + \Delta t^2 \mathbf{a}(t) + \mathcal{O}(\Delta t^4)$$



Imposing External Forces

- Most flows driven by some external force
 - e.g. vibrating wall, pressure gradient, body force
- Need some way to couple in those forces
- Eulerian velocity computed as time average of N_i molecules according to

$$\mathbf{v}(\mathbf{x}) = \frac{1}{N_i} \left\langle \sum_j \frac{d\mathbf{x}_j}{dt} \right\rangle$$

- Stress tensor computed by

$$\boldsymbol{\tau}(\mathbf{x}) = \frac{1}{V_i} \left\langle \sum_j \left[\frac{d\mathbf{x}_j}{dt} - \mathbf{v}(\mathbf{x}) \right] \left[\frac{d\mathbf{x}_j}{dt} - \mathbf{v}(\mathbf{x}) \right] + \sum_{j<i} \mathbf{r}_{ij} \mathbf{f}_{ij} \right\rangle$$



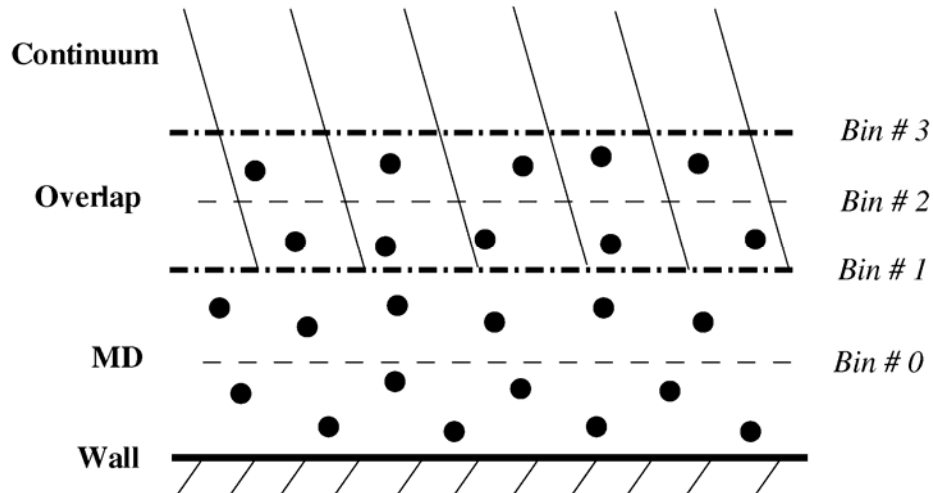
Computational Complexity

- Have to sum over all pairs of molecules so order N^2
- Cut-off distance reduces computational complexity somewhat
- Pairs of interacting molecules stored in *Verlet list*
 - For each molecule $a=1,2,\dots,N$ create a list of neighbors that are within a distance r_c+r_s where r_c is the cut-off distance and r_s is called a *skin thickness*
 - r_s is chosen such that in a time interval of $S \sim 20 \Delta t$, no molecules from outside the skin enter the interaction range of molecule a
- Computational intensity reduced somewhat to (order N) + S^{-1} (order N^2)



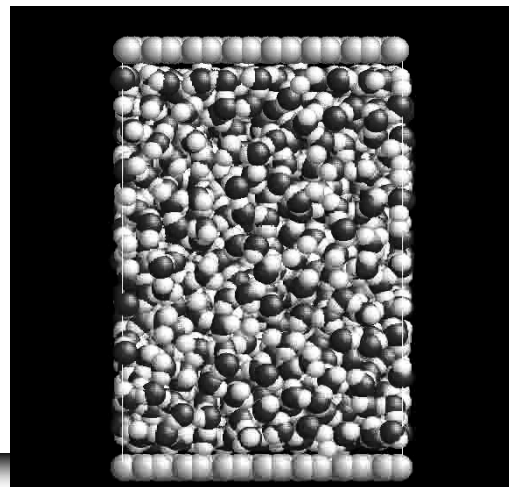
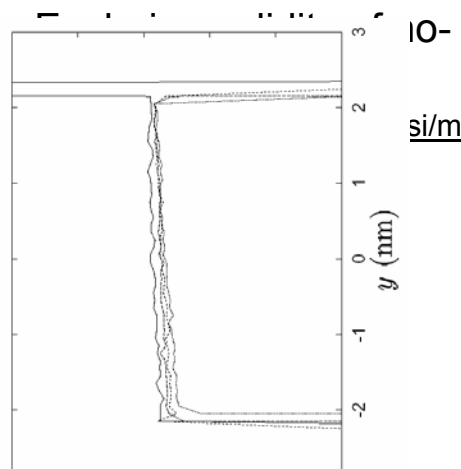
MD/Continuum Approach

- Occasionally desirable to combine MD and Continuum approach (e.g. N-S)
 - For example external flow over a body



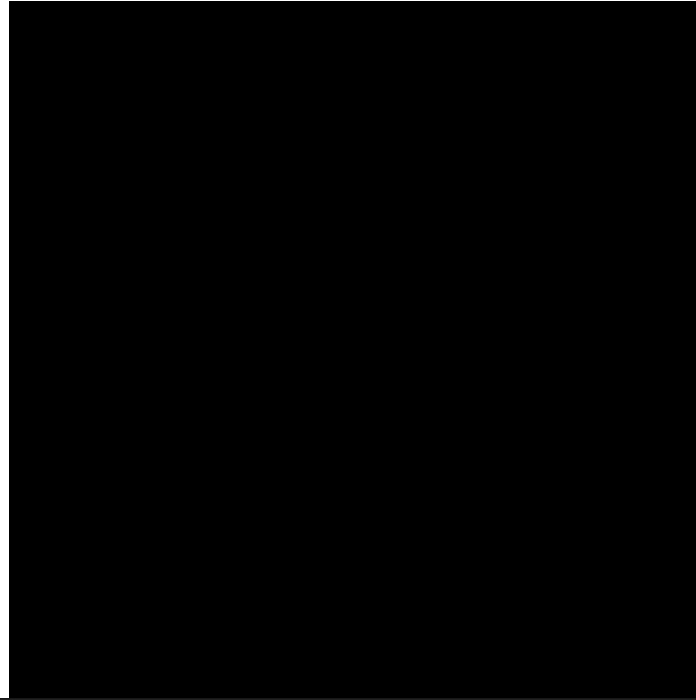
MD: Water Flow between Graphite Sheets

- ETH-Zurich simulated flows in and around CNTs and graphite sheets (Nanotech 2003)



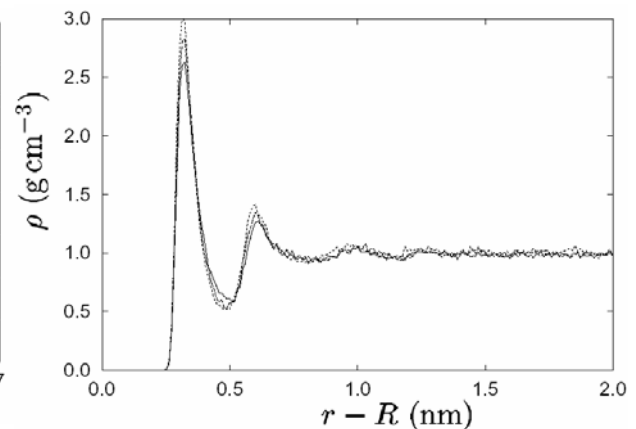
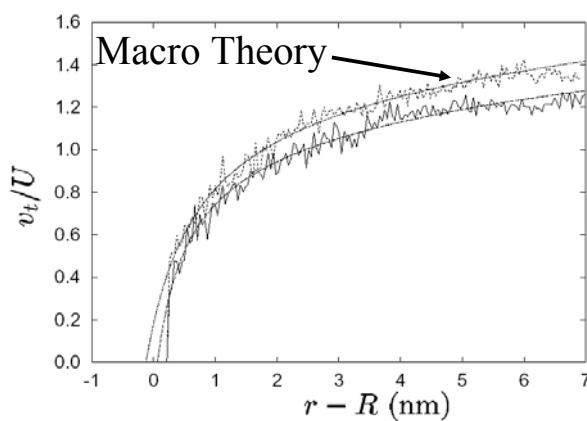
Slip lengths of 14-63 nm
 → No-slip violated

Flow Around CNTs (ETHZ)

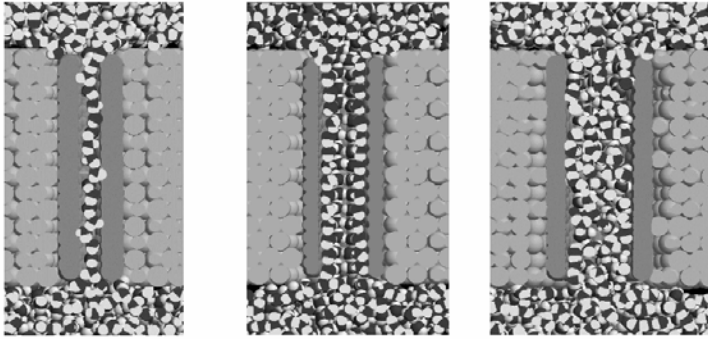


Flow Around CNTs (ETHZ)

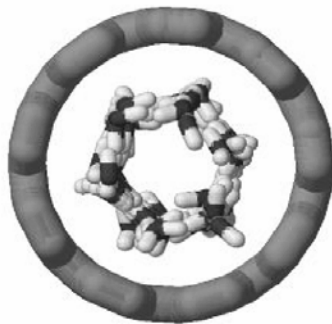
- Flow agrees quite well with continuum theory
- Slip length less than a single molecular diameter
- Considerable variations in fluid density near CNT



Water Ordering in CNTs



- Water passing through CNTs
- Dia=3.1, 8.6, 18.1 Å
- Hexagonal ice-like structure observed in 'liquid water'

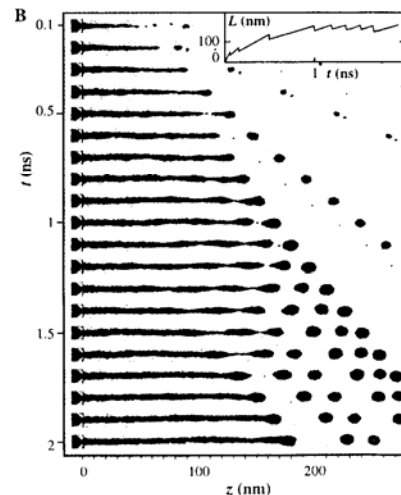
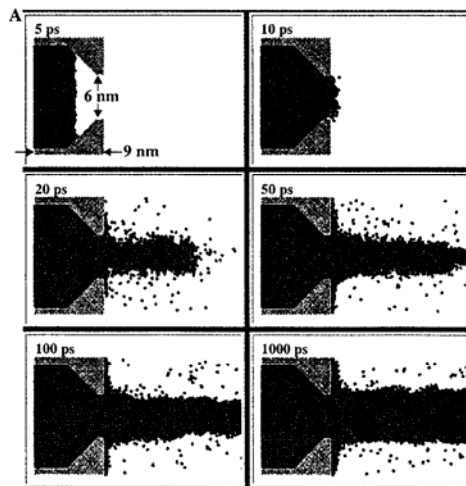


WATER ORDERING BY CONFINEMENT IN CARBON NANOTUBES AT 300K: Mashl, Joseph, Aluru and Jakobsson, Nanotech 2003



Nanojet Breakup using MD

Fig. 1. (A) Atomic configurations selected from MD simulations of a propane NJ formed through injection into vacuum through a convergent 3D gold nozzle with the dimensions given in the top left panel. The upper solid gold walls were removed to expose the interior of the nozzle. A pressure of 500 MPa is applied at the back of the nozzle assembly, the temperature inside the nozzle is controlled at 150 K, and the exterior gold surface of the nozzle exit is heated to 230 K. The sequence of configurations depicts the initial exit of the propane fluid (10 ps) and wetting of the outside surface of the nozzle to form a thin adsorbed propane film, accompanied by swelling of the exiting fluid propane jet near the nozzle exit ($t \geq 20$ ps). The formation of the jet, which achieves a flow velocity of 200 m/s, is accompanied by evaporative cooling and steady-state flow is achieved at ~ 1 ns. The propane molecules are depicted in blue, and the gold atoms are in yellow. **(B)** Evolution of the propane NJ along the direction of propagation (z axis) at selected times ($0.1 \text{ ns} \leq t \leq 2 \text{ ns}$) after exit from the nozzle. Formation of fast-moving droplets and molecular clusters is observed at the initial (transient) stage ($t \leq 1 \text{ ns}$), achieving steady-state flow conditions ($v = 200 \text{ m/s}$)



at $t \approx 1 \text{ ns}$. Molecular evaporation and formation of necking instabilities are observed, resulting in breakup events and formation of drops. At pinch-off, the droplets are of elongated ellipsoidal shape, and they become rounded shortly after. On some occasions, small satellite (secondary) drops are seen (for example, at $t = 1 \text{ ns}$) merging later with the preceding larger drop. In the inset, we display the time evolution of the intact length of the jet. Each sawtooth-shaped discontinuity corresponds to a pinch-off of a drop. At $t \geq 1 \text{ ns}$, steady state is achieved with the mean breakup length of the jet, $L_b \approx 170 \text{ nm}$.



Direct Simulation Monte Carlo (DSMC)

- Developed by G. Bird, circa 1965
- Under standard conditions in a gas there are 10^{10} molecules in a cube measuring $10\ \mu\text{m}$ on a side
 - Not possible to simulate volume this size with MD
- DSMC uses hundreds of thousands or millions of ‘simulated’ molecules that each represent the behavior of thousands of molecules
 - These are typically called ‘particles’
- More approximate technique but achieves results where MD fails



DSMC Overview

- Time is split into steps smaller than the mean collision time
- Space is split into cells proportional to the mean free path
 - In order to adequately resolve spatial velocity gradients, cell size typically taken to be $\Delta x_c \sim \lambda/3$
- Temporally and spatially averaged molecular quantities presented as macroscopic values at cell centers

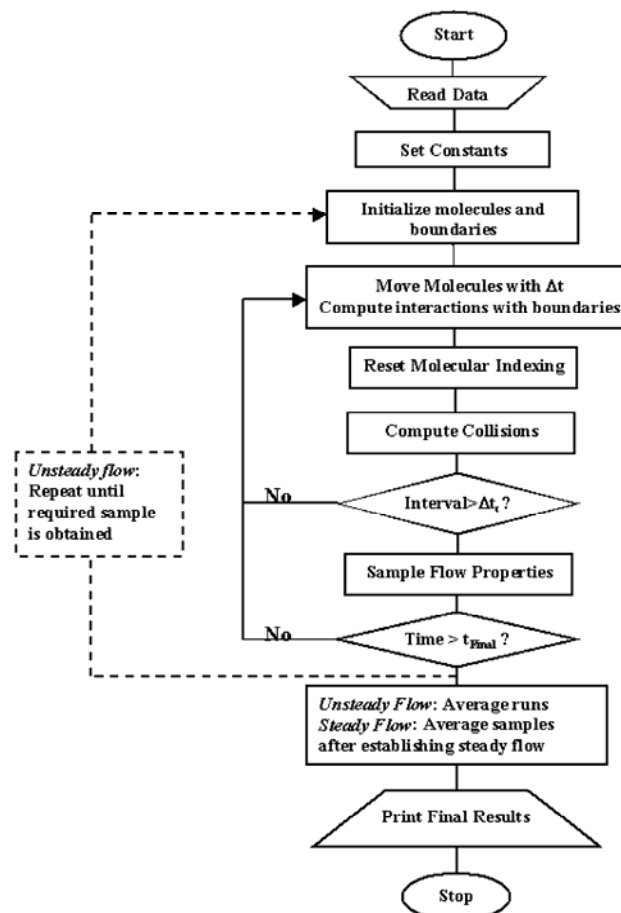


Four main steps in DSMC

- Simulate the motion of particles
 - Each particle has an initial motion
 - Evolve positions forward in time Δt
 - Apply boundary conditions
- Index and cross-reference particles
 - Keep track of which cell each particle is in
 - Keep track of particles that have entirely left computational domain
- Simulate collisions within cells
 - Since motion and collision separated, must use probabilistic approach
 - Calculate new particle velocities
- Sample macroscopic properties of flow



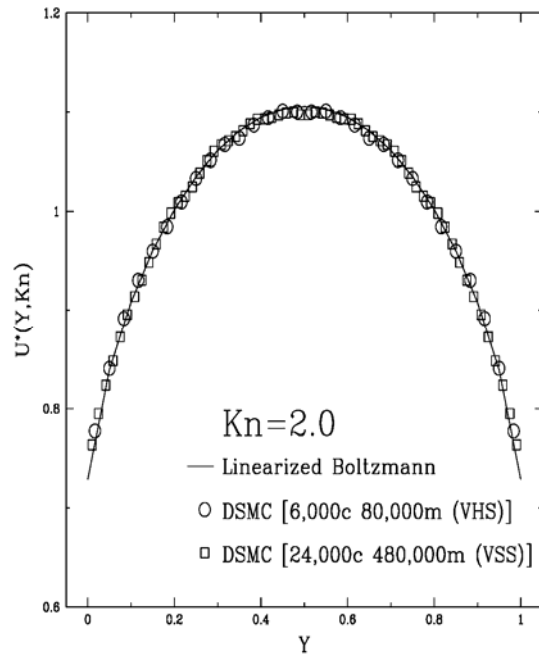
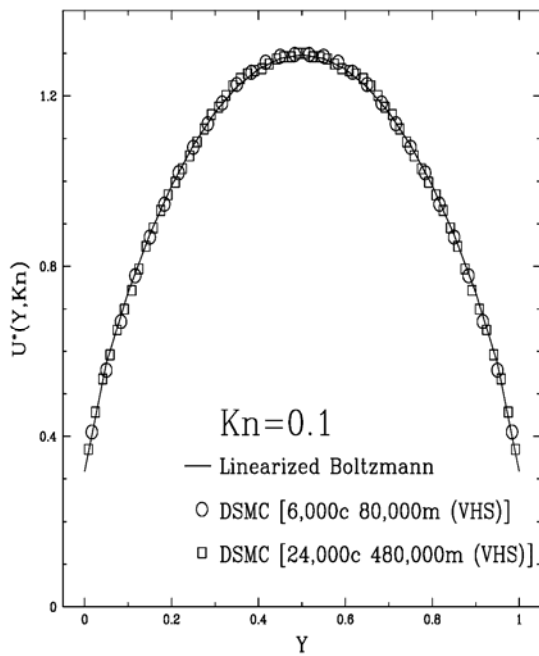
Typical DSMC Flowchart



Beskok, 2002

DSMC versus linearized Boltzmann

Beskok, 2002



ICTP Microfluidics Shortcourse Copyright 2005 by Steve Wereley, Purdue University

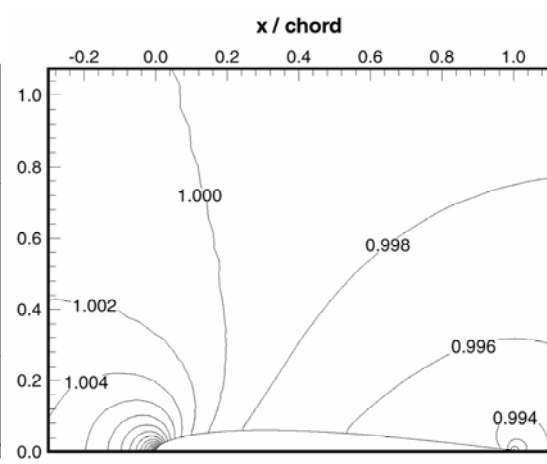
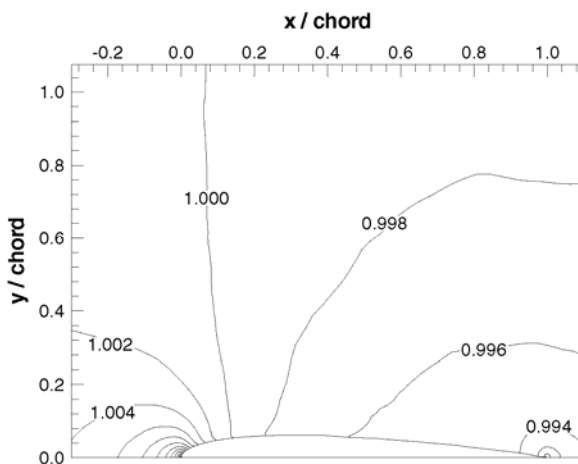


47

Comparison of DSMC and Continuum/Slip

Beskok, 2002

- Flow over a NACA 0012 airfoil with $M=0.1$, $Re=1$, $Kn=0.013$



Continuum approach with a slip boundary condition

ICTP Microfluidics Shortcourse Copyright 2005 by Steve Wereley, Purdue University



48

Limitations of DSMC

- For cell sizes larger than one mean free path, transport quantities (viscosity, thermal conductivity) will deviate from accepted values
- Time step size must be smaller than local collision time t_c
 - Larger times result in particles traveling through many cells without experiencing a collision
- Ratio of simulated molecules to real molecules
 - When this ratio becomes too high, statistical scatter becomes significant
- Boundary conditions may cause problems
 - For example when ΔP is specified for a channel flow, DSMC may predict a different pressure at outlet



Boltzmann Equation

- Can be derived rigorously from Newton's laws and gas dynamics relations for low density gases
- Generally used for the entire Kn regime ($0 \leq Kn < \infty$)
- Describes evolution of a *velocity distribution function* by molecular transport and *binary* intermolecular collisions
- Consider a monatomic gas with velocity distribution given by $f(t, \mathbf{x}, \mathbf{v})$
 - \mathbf{x} represents the position vector
 - \mathbf{v} represents the velocity vector
- This distribution obeys the Boltzmann eq'n



Boltzmann Equation

$$\frac{\partial f}{\partial t} + \mathbf{v} \cdot \frac{\partial f}{\partial \mathbf{x}} + \mathbf{F} \cdot \frac{\partial f}{\partial \mathbf{v}} = Q(f, f_*)$$

where \mathbf{F} represents an imposed body force and $Q(f, f_*)$ represents the effect of intermolecular collisions given by:

$$Q(f, f_*) = \int_{R^3} \int_{S^+} |\mathbf{V} \cdot \mathbf{n}| [f(\mathbf{x}, \mathbf{v}'_*) f(\mathbf{x}, \mathbf{v}') - f(\mathbf{x}, \mathbf{v}_*) f(\mathbf{x}, \mathbf{v})] d\mathbf{n} d\mathbf{v}_*$$

$Q(f, f_*)$ represents the collision of two molecules with post-collision velocities \mathbf{v} and \mathbf{v}_* and pre-collision velocities \mathbf{v}' and \mathbf{v}'_* subject to the following definitions

$$\mathbf{V} = \mathbf{v} - \mathbf{v}_*; \quad \mathbf{v}' = \mathbf{v} - \mathbf{n}(\mathbf{n} \cdot \mathbf{V}); \quad \mathbf{v}'_* = \mathbf{v}_* + \mathbf{n}(\mathbf{n} \cdot \mathbf{V})$$



Boltzmann Equation Terms

$$\frac{\partial f}{\partial t} + \mathbf{v} \cdot \frac{\partial f}{\partial \mathbf{x}} + \mathbf{F} \cdot \frac{\partial f}{\partial \mathbf{v}} = Q(f, f_*)$$

A B C D

- Typical Reynolds Transport Theorem form
- A represents the change in the number of molecules in a region of space
- B represents the molecules convected in or out of a region of space
- C represents the convection of molecules due to the body force, and
- D represents the collision of molecules



Boltzmann Equation

- This equation is solved subject to some constraints
- If we construct quadratic function $\phi(\mathbf{v})$ so that

$$\phi(\mathbf{v}) \equiv a + \mathbf{b} \cdot \mathbf{v} + c|\mathbf{v}|^2$$

- then conservation of mass, momentum, and energy are given by

$$\int_{R^3} \phi(\mathbf{v}) Q(f, f_*) d\mathbf{v} = 0$$

Boltzmann

inequality \rightarrow

$$\int (\log f) Q(f, f_*) \leq 0.$$



Boltzmann Equation

- Macroscopic quantities are calculated according to

$$\rho(\mathbf{x}, t) = m \int f(\mathbf{x}, \mathbf{v}, t) d\mathbf{v}$$

$$\rho \mathbf{u}(\mathbf{x}, t) = m \int \mathbf{v} f(\mathbf{x}, \mathbf{v}, t) d\mathbf{v}$$

$$T(\mathbf{x}, t) = \frac{m}{3nk_B} \int c^2 f(\mathbf{x}, \mathbf{v}, t) d\mathbf{v}$$

$\mathbf{c} \equiv \mathbf{v} - \mathbf{u}$ and is called the *peculiar velocity*, m is molecular mass



Boltzmann Equation

- Solutions are exceedingly difficult
- Require different approaches for various limits
 - Hydrodynamic limit, $Kn \rightarrow 0$
 - Free-molecular limit, $Kn \rightarrow \infty$
 - Transition region (most difficult)



Free molecular gas flow

- For $Kn > 1$, must resort to computations for real problems although analytical solutions exist for very simple geometries
- Beskok (2002) computed many flows in microdomains and determined a generalized relationship for flow in a pipe:

$$\dot{m}_{fm} = \frac{4d^3 \Delta P}{3L} \sqrt{\frac{2\pi}{RT}} \quad \text{where} \quad R = \frac{\bar{R}}{M} \quad \text{where} \quad \bar{R} = 8.3145 \frac{\text{kJ}}{\text{kmol K}}$$

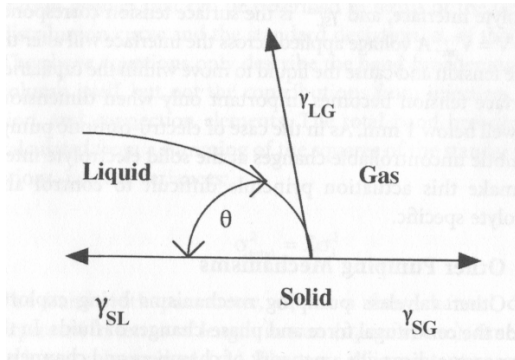
$$\frac{\dot{m}}{\dot{m}_{fm}} = \frac{3\pi}{64Kn_{avg}} \left(1 + \alpha Kn_{avg}\right) \left(1 + \frac{4Kn_{avg}}{1 - bKn_{avg}}\right)$$

for a tube, $\alpha = 1.358$, $b = -1$ consult Karniadakis (2002) for more



Surface Tension

Surface tension (γ) is the increase in energy as the surface area increases.

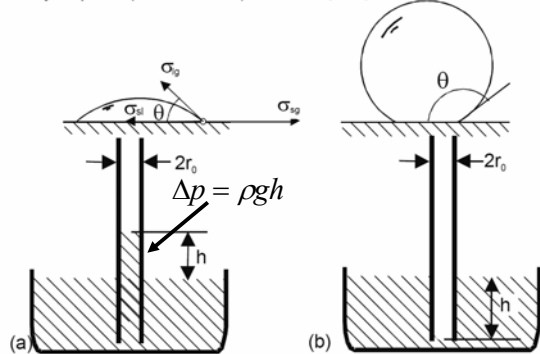


Young's Equation

$$\gamma_{SL} + \gamma_{LG} \cos \theta = \gamma_{SG}$$

Hydrophilic ($0^\circ < \theta < 90^\circ$)

Hydrophobic ($90^\circ < \theta < 180^\circ$)



$$\Delta p = \frac{2(\gamma_{SG} - \gamma_{SL})}{r} = \frac{2\gamma_L \cos \theta}{r}$$

$$\gamma_{\text{water}} = 72.8 \text{ mN/m}$$

$$r = 10^{-6} \text{ m}$$

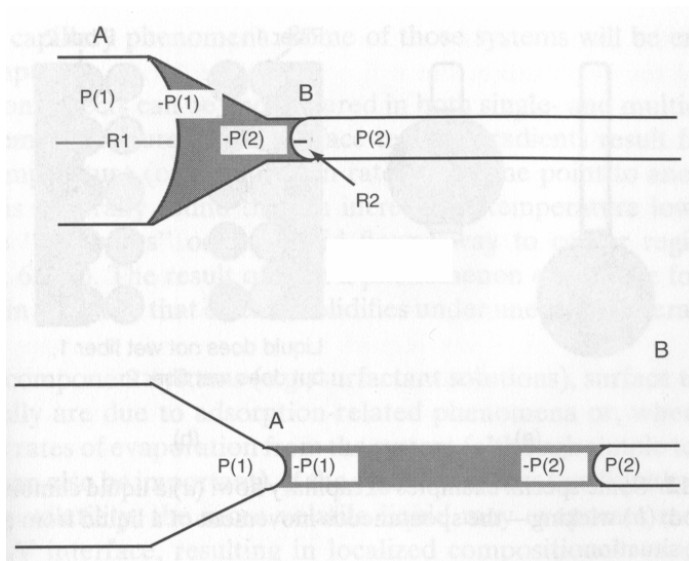
$$\Delta p \sim 100 \text{ kPa or 1 atm}$$

Capillary force driven pumping: (a) hydrophilic; and (b) hydrophobic.



Surface Tension

Capillary tube wetting



Unstable

Stable = Stuck!

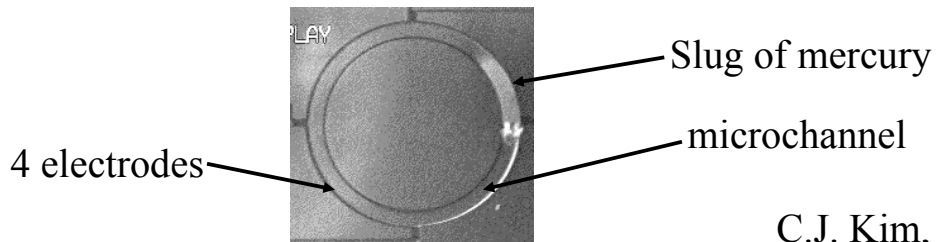


Electro-Wetting

- Based on changing surface tension by applying a potential to an interface

$$\gamma_{SL} = \gamma_{SL}^{\max} - \frac{\epsilon_r \epsilon_0}{2\delta} (V - V_{pzc})^2$$

- Change in voltage across an interface produces a change in surface tension



C.J. Kim, UCLA

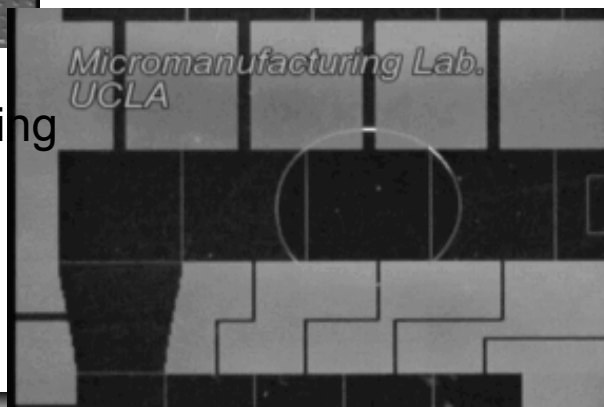


Other Electrowetting Examples (CJ Kim, UCLA)



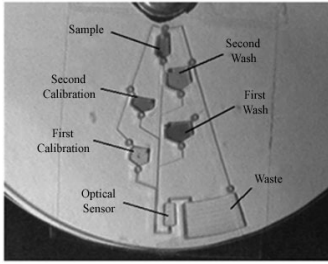
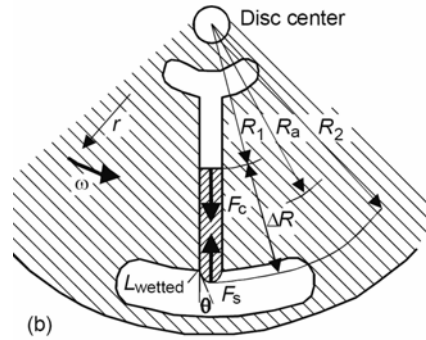
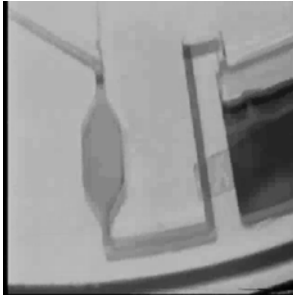
- Droplets moving around a planar surface

- Splitting and combining droplets/mixing



Centrifugal Forces

Lab-on-a-Disk: Marc Madou, UC-Irvine



Centrifugal Force: $\frac{dF_c}{dr} = \rho \omega^2 r$

Surface Tension: $F_s = \frac{\sigma \cos \theta L_{\text{wetted}}}{A}$

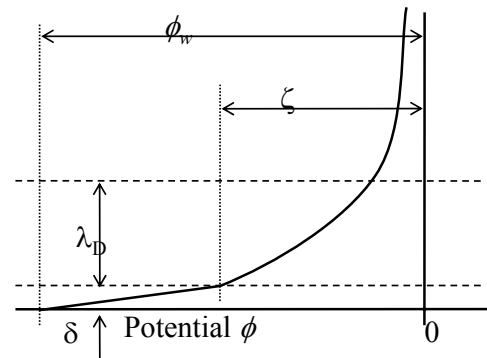
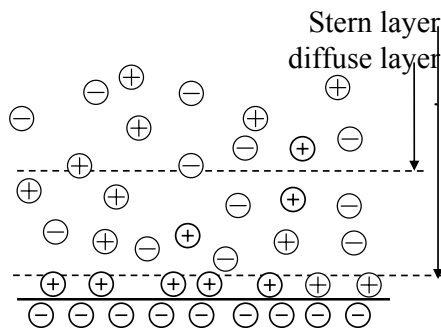
Burst Frequency: $f_b \geq \sqrt{\frac{\sigma \cos \theta}{\pi^2 \rho R_a \Delta R D_h}}$



Electrokinetics

- Most surfaces acquire surface charge in presence of polar liquid

- e.g. glass-water
- many polymers and water, too
- Debye thickness generally order of nm
- $K = 1.3805 \times 10^{-23} \text{ J/K}$, $F = 9.65 \times 10^4 \text{ C mol}^{-1}$, $\lambda_D = \sqrt{\frac{\epsilon K T}{2 z^2 F^2 c_\infty}}$
 z is valency of ion, c_∞ is bulk concentration, ϵ is permittivity ($8.85418 \times 10^{-12} \text{ F/m}$ for vacuum)



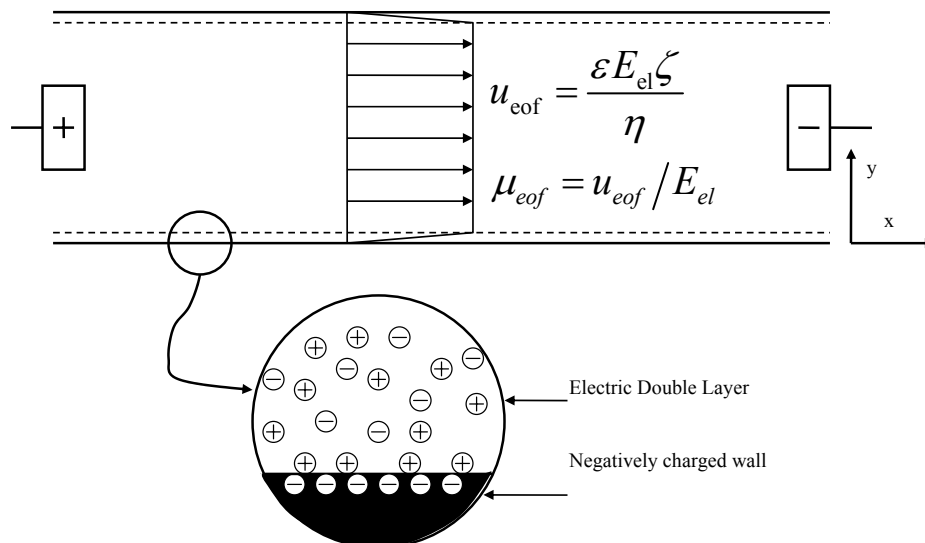
Classifications of Electrokinetic Flows

Name	Type of Movement	Electrokinetic Coupling
Electrophoresis	Charged surface moves relative to a stationary liquid	Use an applied electric field to induce movement
Electroosmosis	Liquid moves relative to a stationary charged surface	
Streaming Potential	Liquid moves relative to a stationary charged surface	Use movement to create and electric field
Sedimentation Potential	Charged surface moves relative to a stationary liquid	



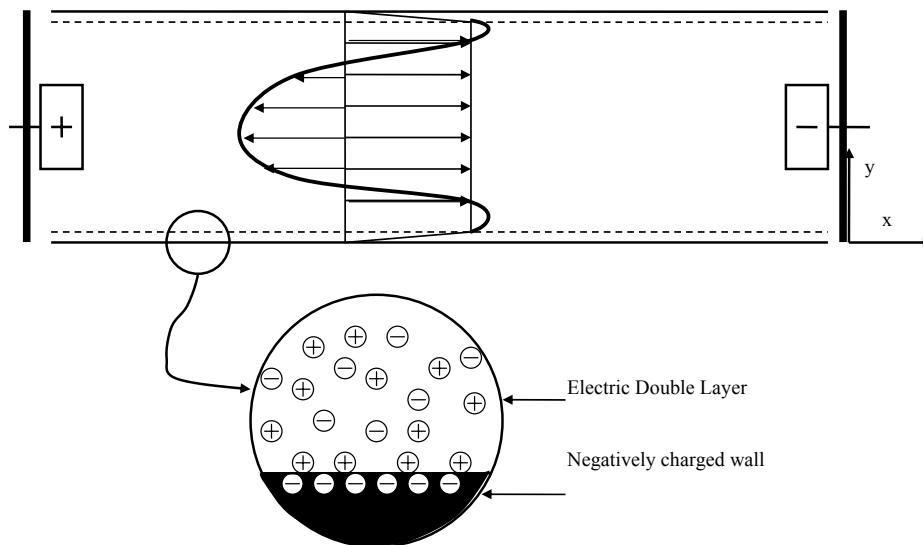
Electroosmosis

- Apply electrical field across channel
- EDL drawn toward electrode pulling bulk along
- “Plug flow” if no pressure gradient



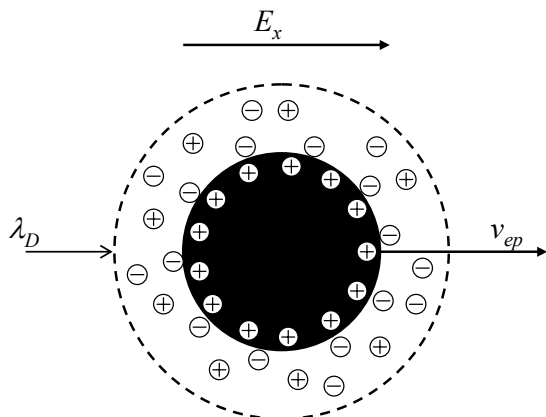
Electroosmosis

- Backflow in the presence of pressure gradient
- Zero mean flow in closed channel



Electrophoresis

- Particle/ion manipulation using EDL and electrical field
 - Common technique called ‘capillary electrophoresis’ (CE) used to sequence DNA, ala OJ Simpson or Human Genome Project



$$u_{ep} = \frac{2}{3} \frac{\epsilon \zeta E_{el}}{\mu}, \lambda_D \ll d_p$$

$$u_{ep} = \frac{\epsilon \zeta E_{el}}{\mu}, \lambda_D \gg d_p$$

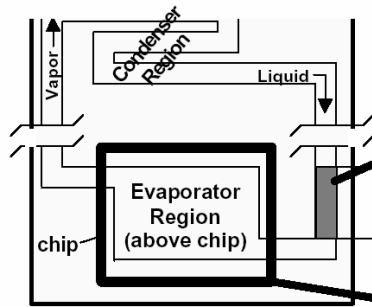
$$\mu_{ep} = u_{ep} / E_{el}$$



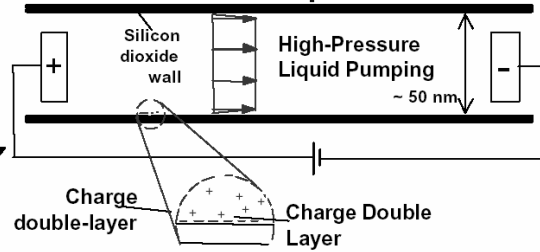
Application: Micro heat exchangers

Kenny, Goodson, Santiago, Cho—Stanford

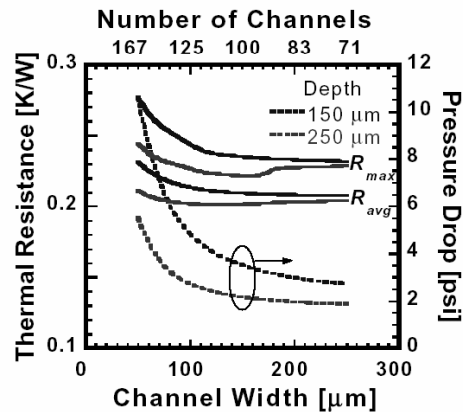
Two-Phase Cooling Loops using Electrokinetic Liquid Pumping



Electrokinetic Pumps



- No solid moving parts -> compact & reliable
- High liquid pressures (> 5 atm) enable two-phase micro heat exchangers
- Voltage controlled
- High peak heat removal rates



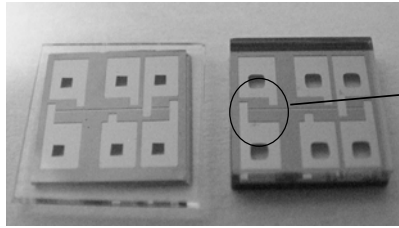
Microdomain Practicalities

- Many microfluidic MEMS operate in simple flow regimes
 - Low Reynolds number
 - Large length scales (compared to molecules)
- Even so, behavior significantly different
 - Flow geometries different
 - Entrance length different
- Let's look at a few examples...

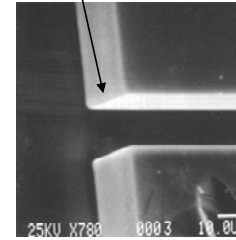
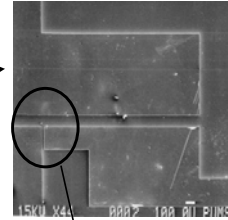
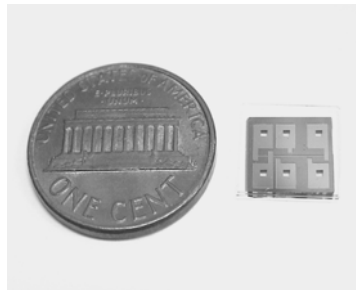


Microscale Mass Flow Meter

Jang, Zhao, Gui, Wereley, Purdue ME



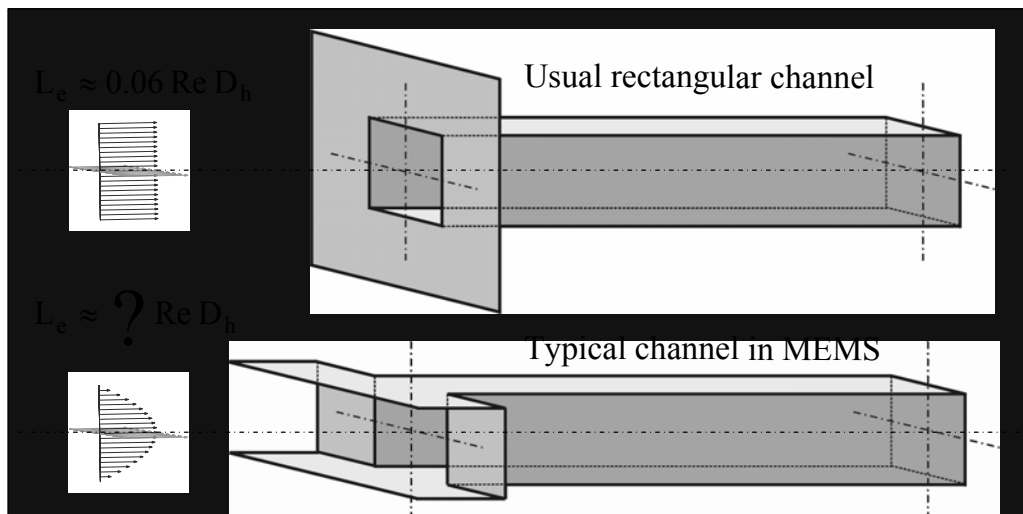
Completed chips made by each of the two processes.



SEM photographs due to the Deep RIE along the microchannel (a) and at the intersection of the microchannels and connecting channels (b)

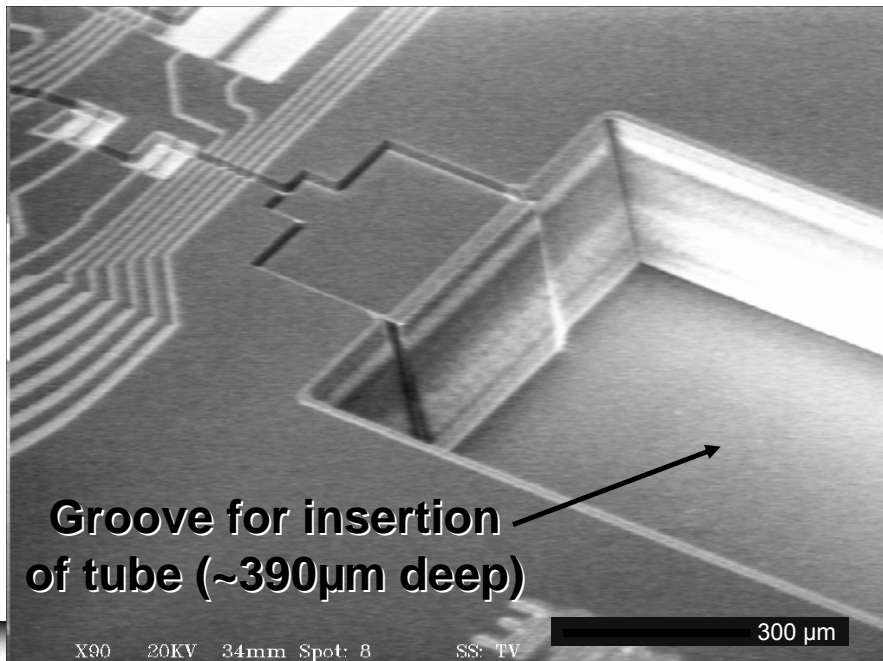


Entrance Length Effects in Micro Channels



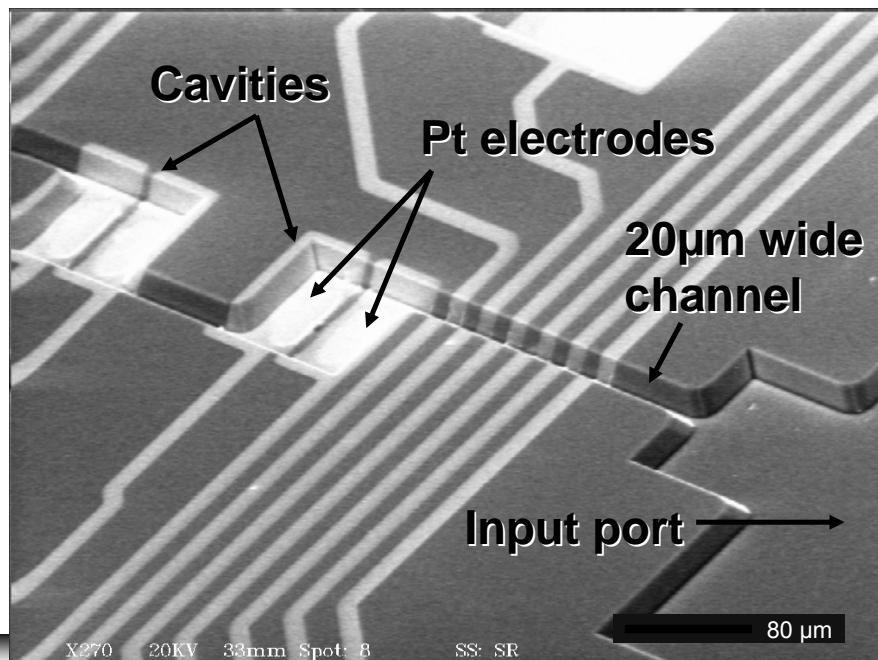
Biomedical Microdevice—Biochip

Bashir and Gomez, Purdue, ECE



Biomedical Microdevice—Biochip

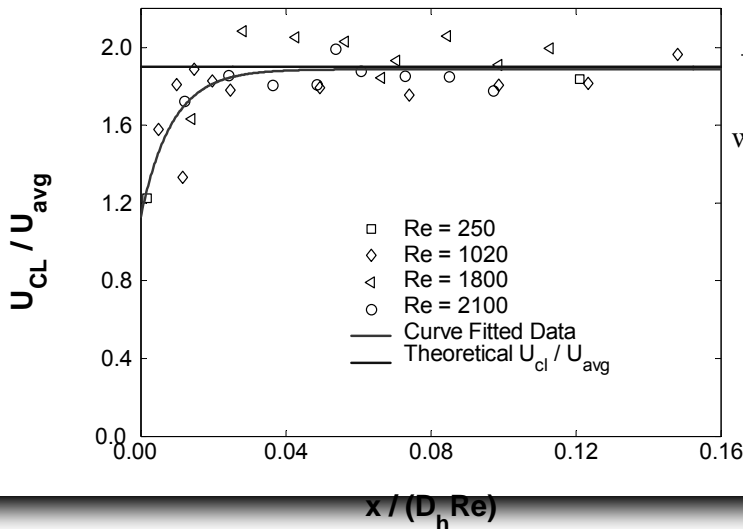
Bashir and Gomez, Purdue, ECE



Entrance Length for Modified Entrance

Lee, Gui, Wereley, Proc. ASME, 2002

- Existing theory predicts: $L_e/D_h \approx C_1 + C_2 Re_{D_h}$, where $C_1 \approx 0.5$ and $C_2 \approx 0.05$ (Shah and London, 1978)



$$\frac{U_{CL}}{U_{avg}} = \left(\frac{U_{CL}}{U_{avg}} \right)_{fd} - A \exp\left(-B \frac{x/D_h}{Re}\right)$$

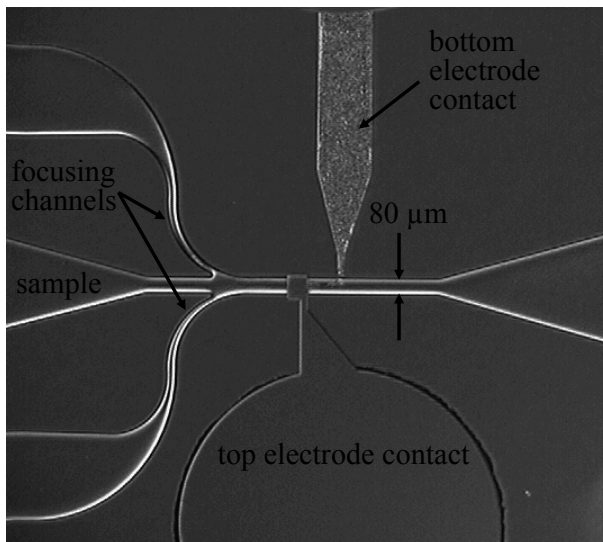
where $A \approx 0.74$ and $B \approx 110.4$

$$C_e = \frac{L_e / D_h}{Re_{D_h}} \approx 0.033$$

45% reduction as compared to existing theory



Microfabricated Particle Impedance Sensor Krulevitch (LLNL), Gasgoyne (MD Anderson CC)



- horizontal sheath flow
- optimized electrodes: uniform E-field
- channels grounded



Modeling of Hydrodynamic Focusing Effect

- Inertial effect: particle velocity lags fluid velocity

- Saffman equation: $f_{\text{lift}} = 81.2\rho_F v^{1/2} V_z a^2 \Gamma^{1/2}$

f_{lift} = hydrodynamic lift force

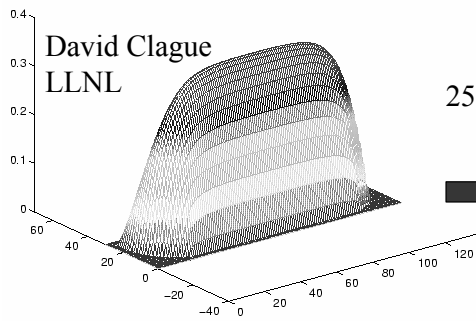
ρ_F = fluid density

v = fluid viscosity

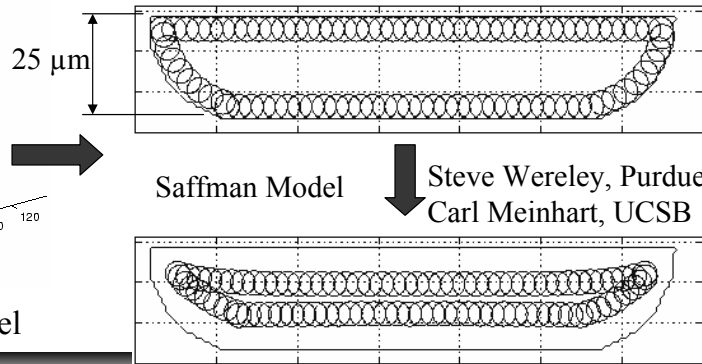
V_z = ave. fluid velocity

a = particle radius

Γ = shear force (rate)



Velocity Profile in μ -Channel



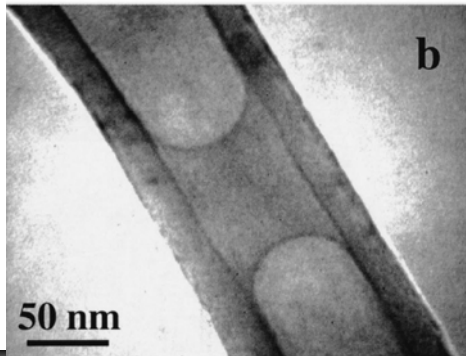
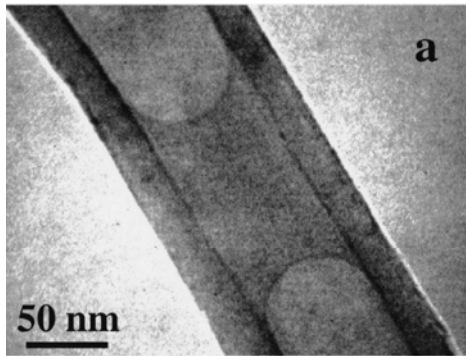
Experimental Characterization of Microflows

1. Transmission Electron Microscopy
2. X-Ray Microimaging
3. Molecular Tagging Velocimetry
4. Particle Image Velocimetry
 1. Measurement of Surface Location
 2. Measurement of Temperature



Water in Carbon Nanotubes

Megaridis, Phys. Fluids, Vol. 14, pp L5-L9, 2002



- Hydrothermally produced multi-wall carbon nanotube
- Water inside nanotube
- TEM micrographs of meniscus
- Water volume decreases from a to b upon heating
- Explanations:
 - Bubble expansion
 - Liquid evaporation
 - Thermocapillarity
- Results inconclusive



Microflow Diagnostic Intro

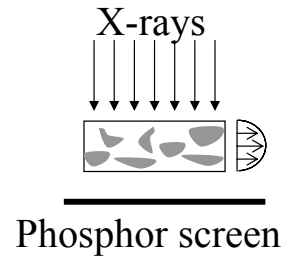
- Need for Microfluidic Diagnostics
 - Even though $Re \ll 1$, flows still complicated
 - Large surface roughness
 - Imprecise boundary conditions
 - Two-phase, non-Newtonian fluids
 - Coupled hydrodynamics and electrostatics equations
 - Non-continuum effects
- Experimentally Unfriendly Environment
 - Limited optical access
 - Seed particles smaller than wavelength of light
 - Brownian motion of seed particles
 - Large background reflections



X-ray Microimaging

Lanzillotto, et al., *Proc. ASME*, 1996, AD52, 789-795.

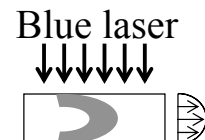
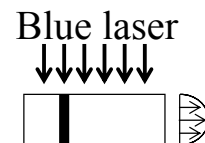
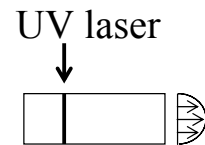
- Positives
 - Can image inside normally opaque devices
- Negatives
 - low resolution $\sim 20\text{-}40\mu\text{m}$
 - depth averaged (2-D)
 - requires slurry to scatter x-rays
 - requires collimated x-rays



Molecular-Tagging Velocimetry

Paul, et al., *Anal. Chem.*, 1998, **70**, 2459-2467.

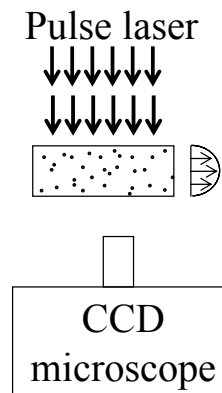
- Positives
 - minimally intrusive
 - better with electrically-driven flows
 - works with gas or liquid flows
- Negatives
 - low resolution $\sim 20\text{-}40\mu\text{m}$
 - depth averaged (2-D)
 - greatly affected by diffusion
 - must invert convection eq.



Micro-Particle Image Velocimetry(μ -PIV)

Santiago, et al., *Exp. Fluids*, 1998, 25(4), 316-319.

- Positives
 - high resolution $\sim 1 \mu\text{m}$
 - small depth average $\sim 2\text{-}10 \mu\text{m}$
 - minimally intrusive
- Negatives
 - requires seeding flow
 - particles can become charged



Overview of X-Ray Microimaging Procedure

- Assume translation and rotation of infinitesimal material particles (assumes incompressibility)
- Enforce smoothness of velocity field
- Two constraints combined as

$$\min \left\{ \iint_R \left[\lambda \left(\frac{DI}{Dt} \right)^2 + \|\nabla \mathbf{u}\|^2 \right] d^2 \mathbf{x} \right\}$$

- where $I(\mathbf{x})$ is image intensity function, λ is a control parameter,
- Apply boundary conditions
 - No-penetration B.C. at surfaces



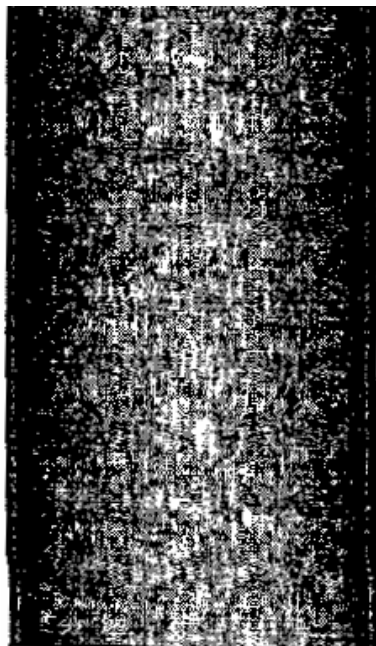
X-Ray Microimaging Solution Procedure

- Jacobi relaxation scheme
- Solution continually varied until constraint minimized
- Solved on grid that is progressively refined from low spatial resolution to high
- Does not assume fluid model
- Choice of parameter λ determines how much variation is allowed between grid points
 - Improper choice can artificially suppress spatial gradients or turbulent structures in flow



X-Ray Microimaging Images

– Raw Image



Calculated Velocity



Lanzillotto, 1996



X-Ray Microimaging Results

- Flow of X-Ray emulsion in quartz capillary
- Tube diameters from 640 to 1000 μm
- Flow rates 4-8 nanoliters/sec
- exposure time: 500 ms

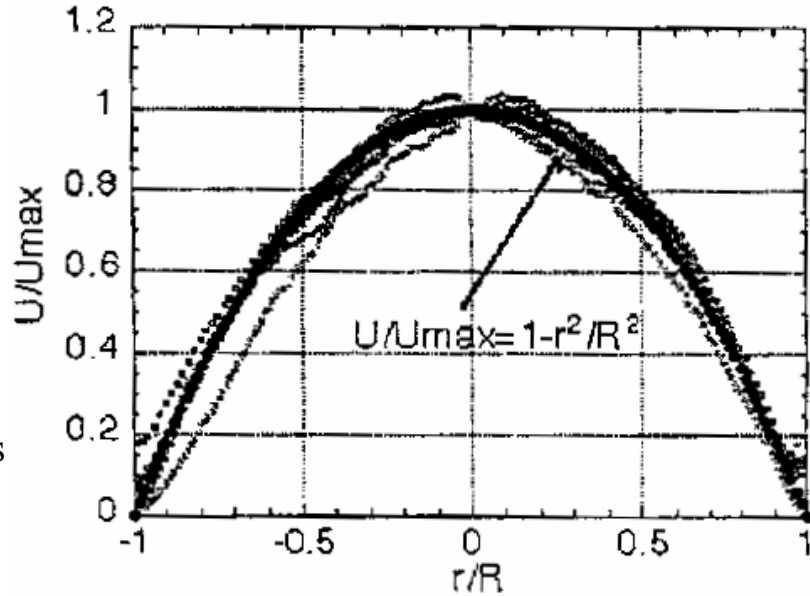
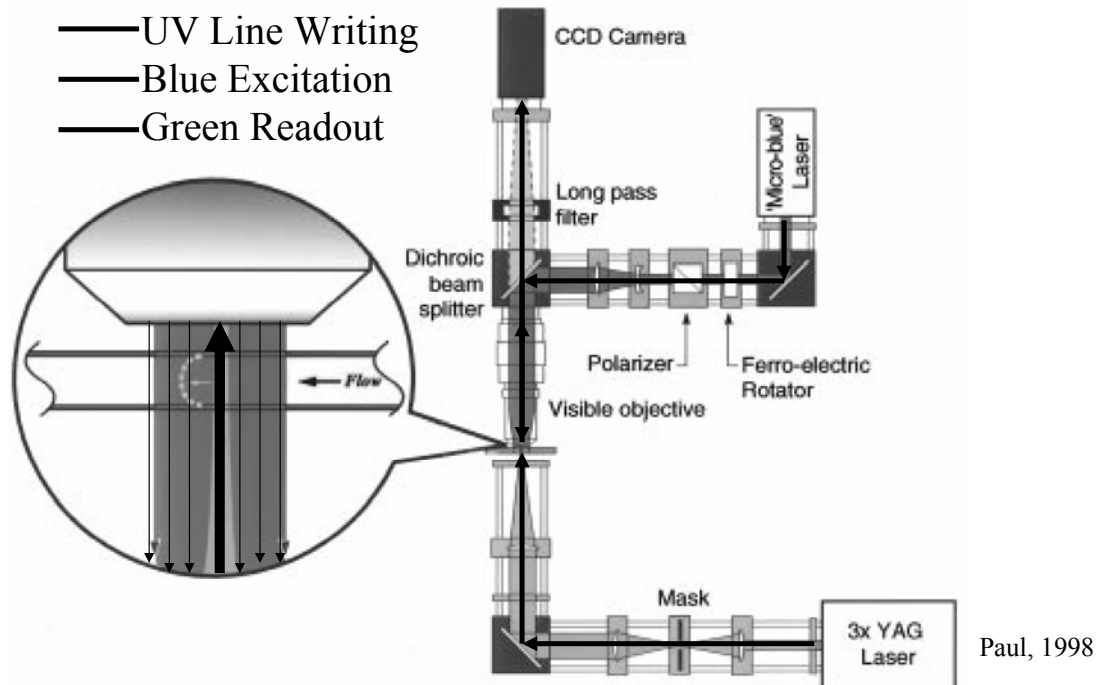


Figure 7. Nondimensional average velocity profiles experimental versus theoretical (solid line)

Lanzillotto, 1996



Liquid MTV

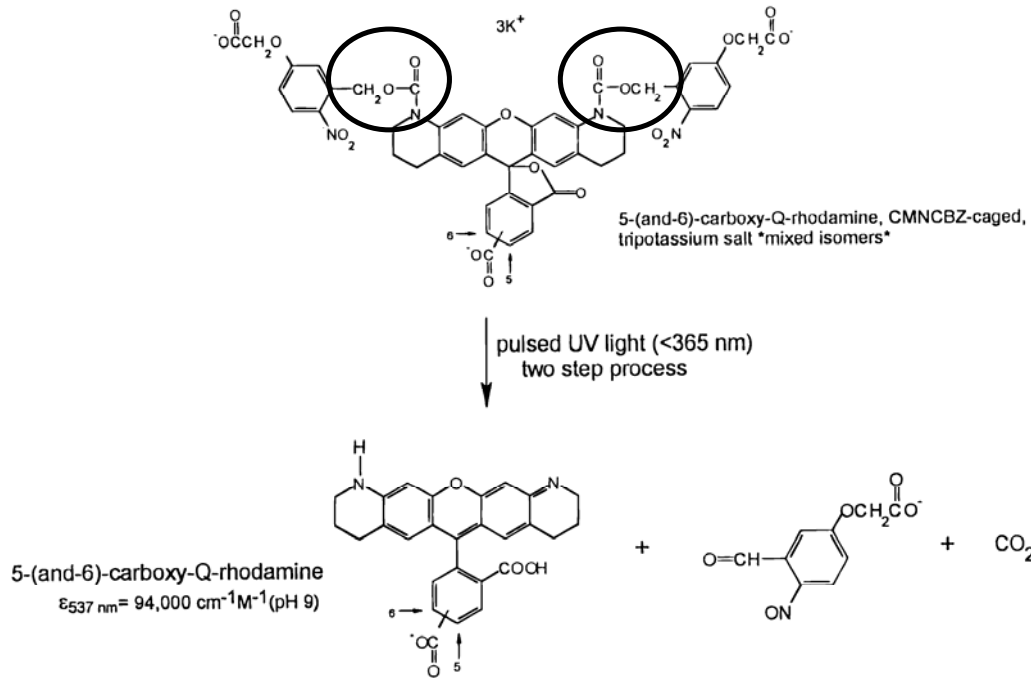


Paul, 1998



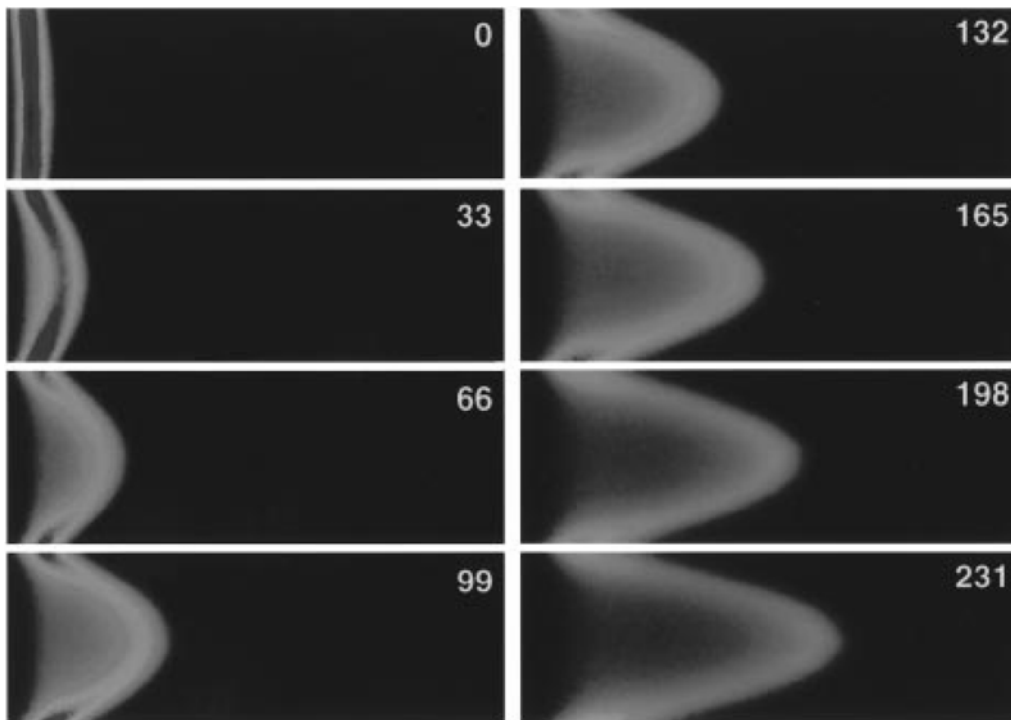
Liquid MTV (Paul, et al.)

Paul, 1998



Liquid MTV (Pressure-driven flow)

Paul, 1998



Liquid MTV

- Original mark in fluid looks like

$$C(t=0, r, z) = \exp(-(z/\sigma)^2)$$

- Evolves in time according to convection diffusion equation

$$\frac{\partial C}{\partial t} + \vec{u} \cdot \nabla C = D \nabla^2 C$$

- For the case of negligible diffusion, time evolution of mark looks like

$$C(t, r, z) = \exp(-(z - u(r)t)^2 / \sigma^2)$$



Liquid MTV

- Methods of recovering the velocity field:
 - Connect the dots
 - Use approximate version of convection diffusion eq'n

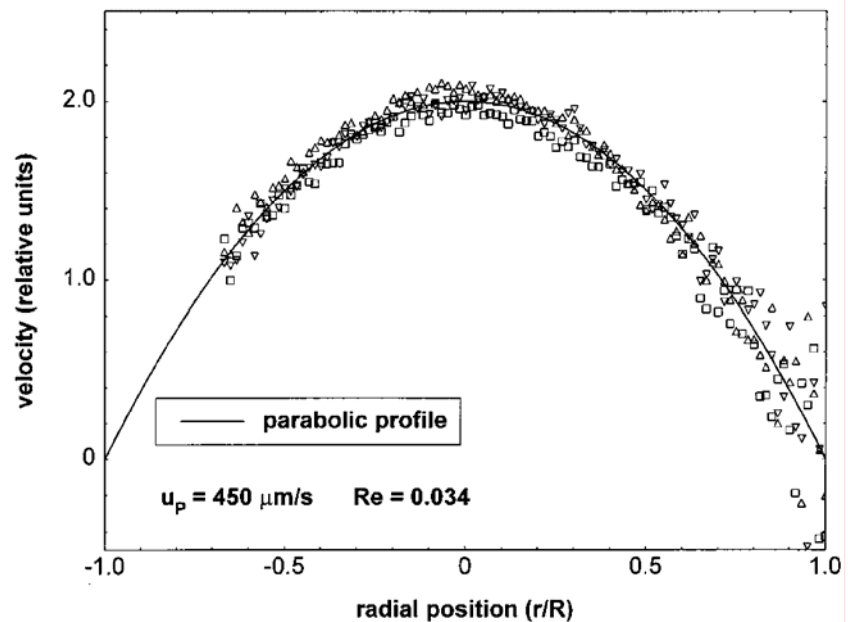
$$u(r) \approx (C(t_0 + \delta t) - C(t_0)) / \nabla C(t_0)$$

- These techniques work for flows with much symmetry
- For more complicated flows, must add in incompressible conservation of mass equation as additional constraint



Liquid MTV Results

- DI water flow in 75 μm cap.
- Good results in center of channel

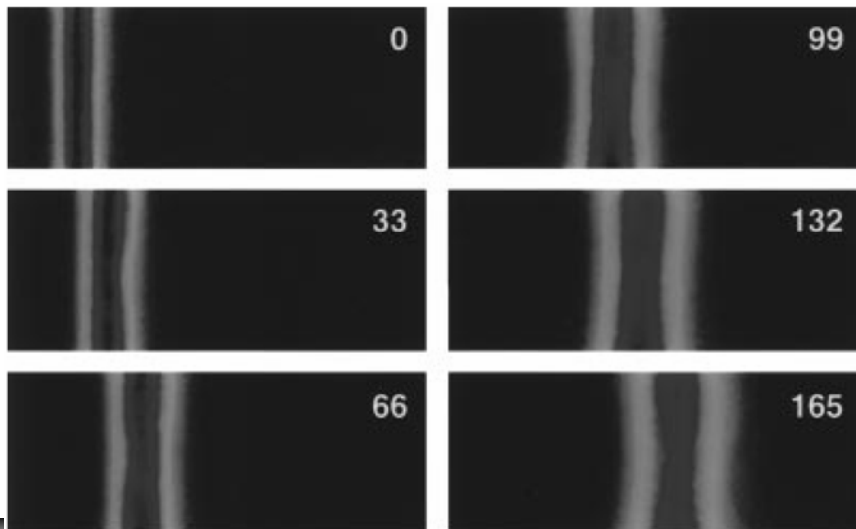


Paul, 1998



Liquid MTV in electrically driven flows

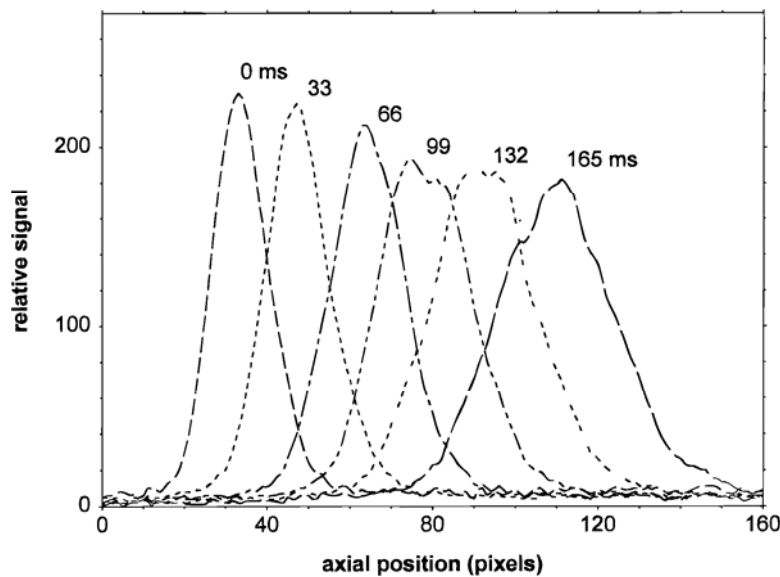
- Electroosmotically driven flow
- Shows potential for resolving slip B.C.s



Paul, 1998



Liquid MTV data interrogation



Paul, 1998



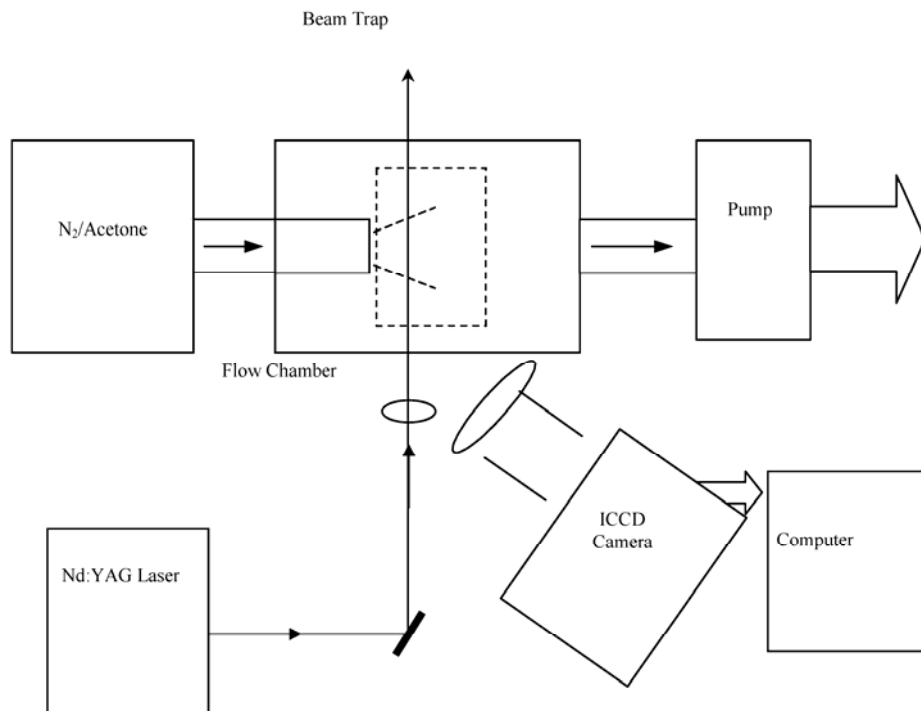
Gas MTV (Lempert, et al.)

- Measured velocity outside of supersonic 'milli nozzle' with exit diameter of 1 mm
- Very similar procedure to liquid MTV
 - Data analysis routines are similar/identical
 - Necessary changes in speed of process and tracer molecules
- Biacetyl molecule
 - Absorbs at 405 nm
 - Fluorescence lifetime up to 1 ms
- Acetone molecules used as tracers
 - Absorbs at 230-340 nm
 - Lifetime on the order of 200 ns



Gas MTV

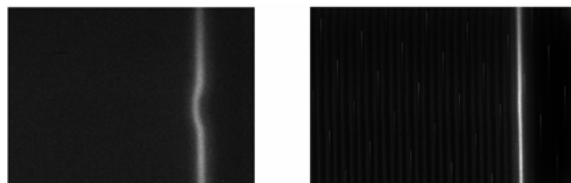
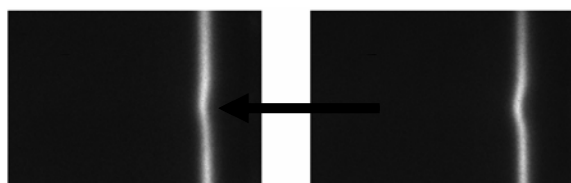
Lempert, 2001



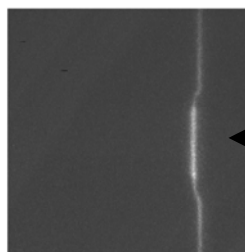
Gas MTV

Lempert, 2001

- Operating at design conditions (pressures matched)

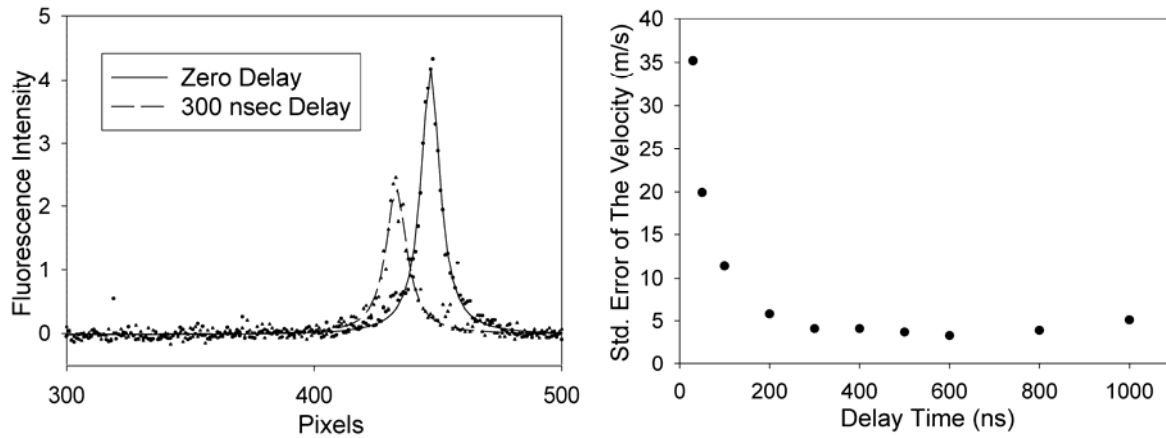


- Severely underexpanded condition



Gas MTV

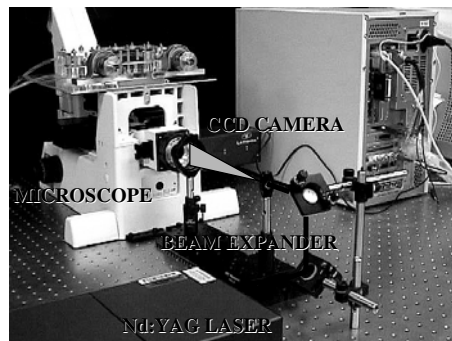
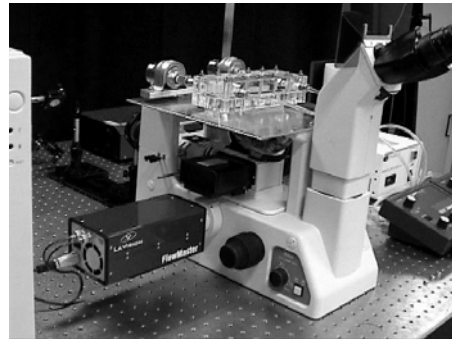
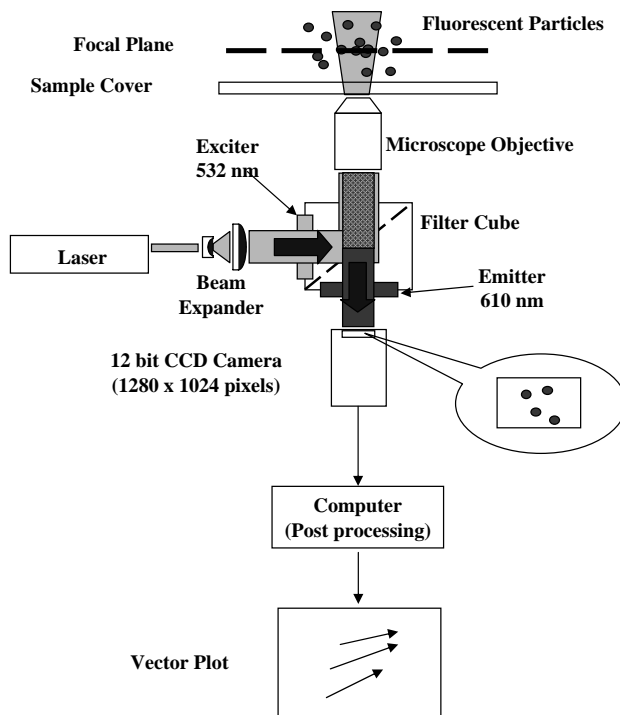
Lempert, 2001



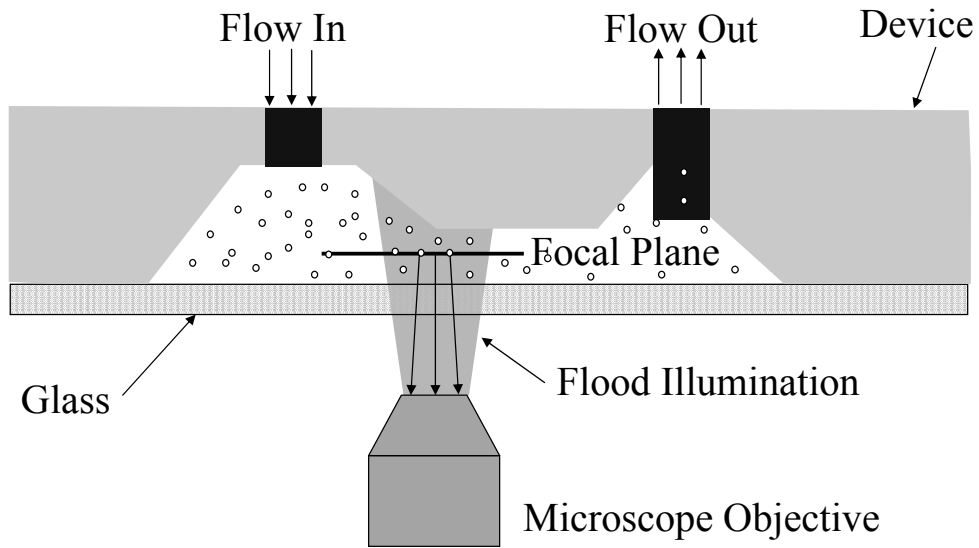
- Left figure cross section of preceding profiles
- Right figure variation of error with time delay



Micro-PIV Schematic and Photos

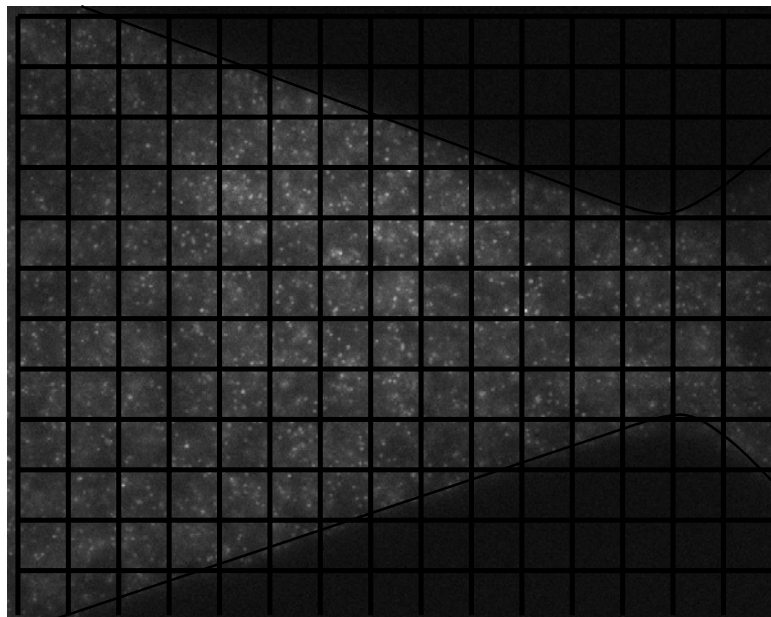


Micro-PIV Schematic

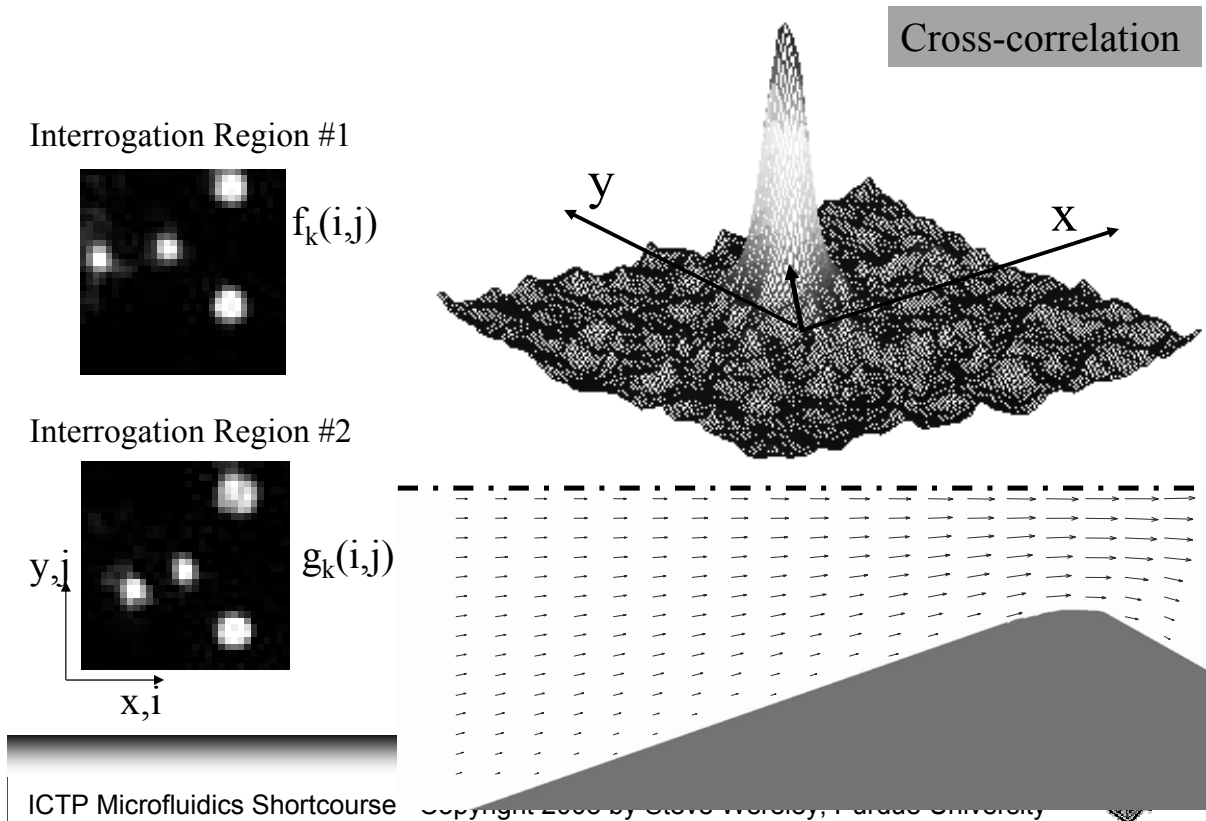


Typical Micro-PIV Image

Microthruster: Magnification 40x, particle size 700 nm
courtesy of K. Breuer, Brown University



Cross-Correlation PIV



Calculating correlation function

- Correlation function can be calculated by direct multiplication and summation
- Or, it can be calculated using a numerical shortcut of working in frequency space, namely

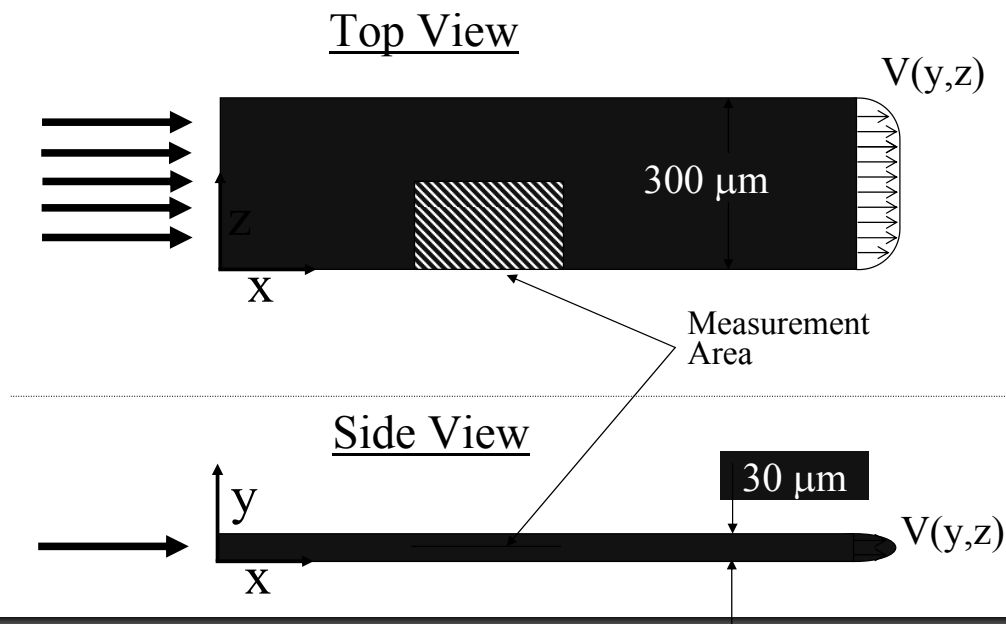
$$\Phi_k(m,n) = \text{fft}^{-1} \left\{ \text{fft}(f_k(i,j)) \times \text{conj}(\text{fft}(g_k(i,j))) \right\}$$

- Greatly increases speed of computation
- Assumes periodicity of f_k and g_k
 - Implies that most of the large correlation peak must lie with the center quarter of the interrogation function or it will be 'folded' over by the Nyquist criterion

Finding peak of correlation function

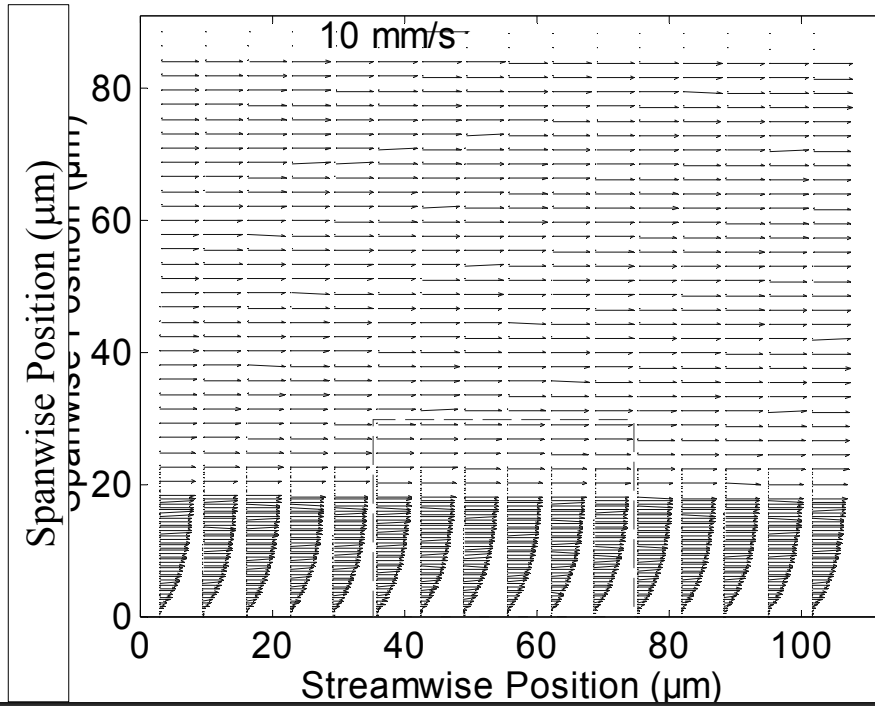
- Several competing methods
- Simplest maximum function
 - Limitation: resolution limited to one pixel
- Centroid
 - Benefit: No presumed peak shape
 - Limitation: Tends to have significant peak locking
- Gaussian
 - Particle images are well modeled by Gaussian function
 - Been shown to be most accurate
 - Typically 3 points used in the x and y direction to determine peak location
 - Accuracies as high as 0.01 pixels

Microchannel Experiments



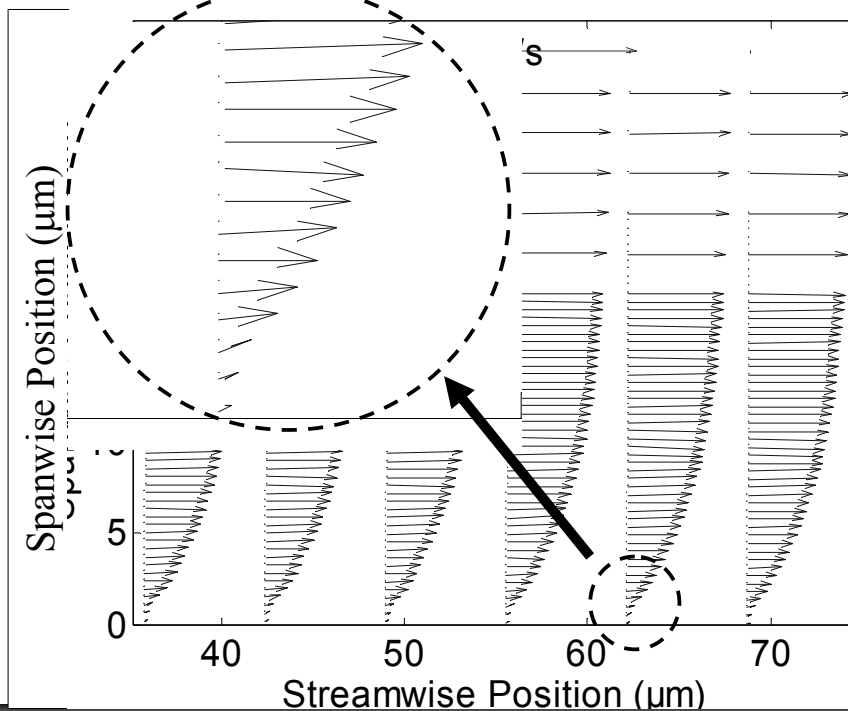
Microchannel Flow (x-z plane)

$y=7\mu\text{m}$ from bottom of channel



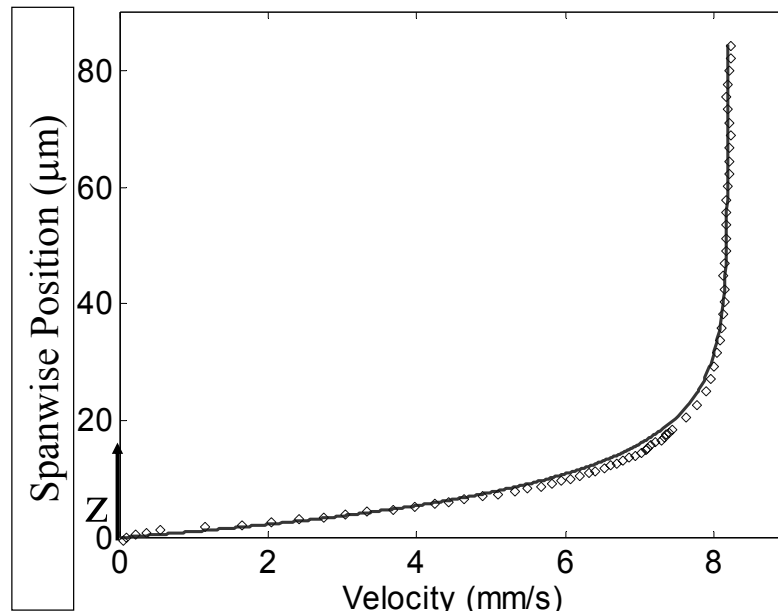
Microchannel Flow (x-z plane)

$y=7\mu\text{m}$ from bottom of channel



Streamwise Profile (x-z plane)

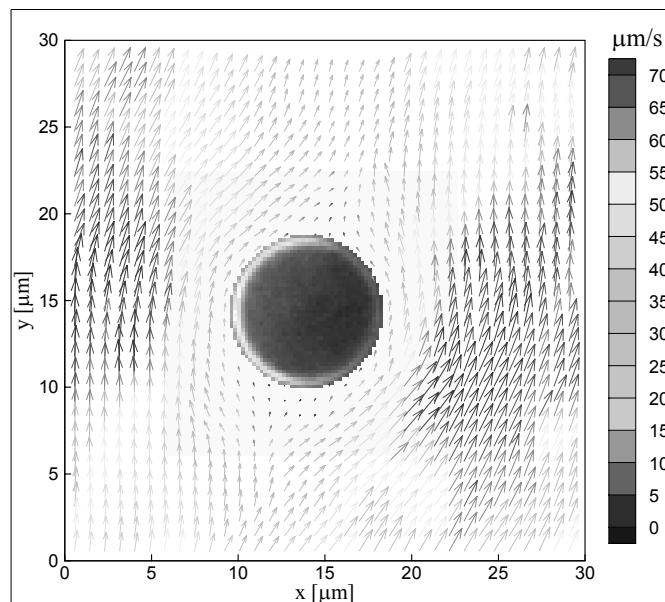
C.D. Meinhart, S.T. Wereley, and J.G. Santiago, "PIV Measurements of a Microchannel Flow," *Exp. Fluids*, Vol. 27, No. 5, 414-419, (1999).



Flow Around a Red Blood Cell

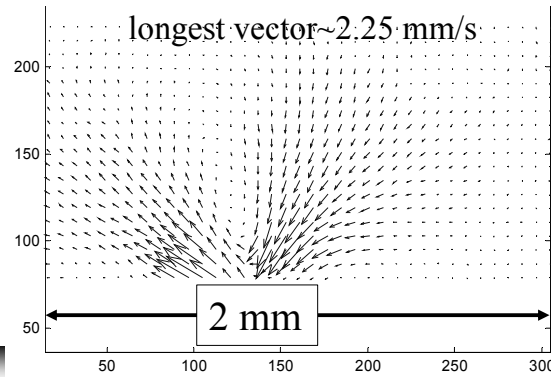
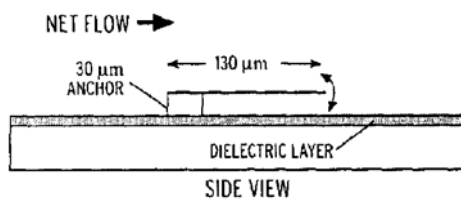
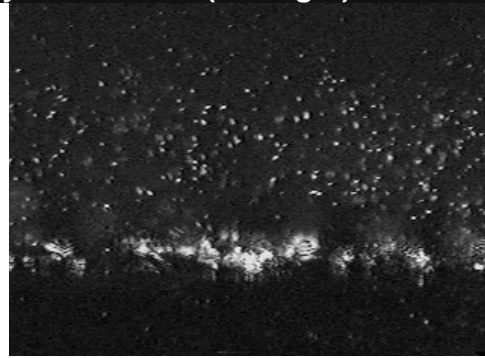
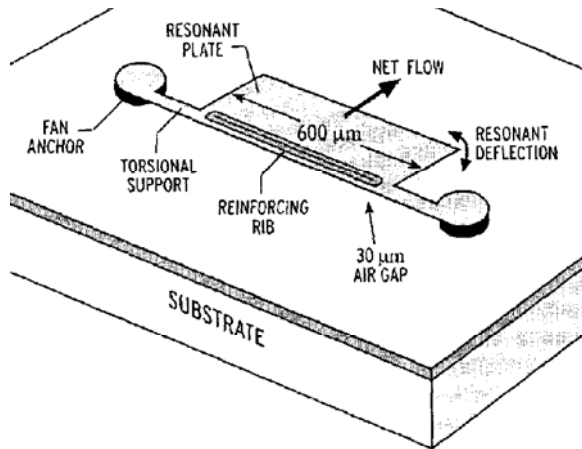
S.T. Wereley and C.D. Meinhart, "Adaptive Second-Order Accurate Particle Image Velocimetry," *Exp. Fluids* (2001).

- Correlation-based interrogation
- Central difference image correction
- Mask technique
- Average correlation method
- Interrogation window: 16×16-pixel
- Spatial resolution: 3.5×3.5×2 μm³
25 zepto liters



Microcantilever driven flow

collaboration with University of Colorado (V. Bright)



ICTP Microfluidics Shortcourse Copyright 2005 by Steve Wereley, Purdue University



Measuring Temperature with Micro-PIV

- without flow
- with flow

ICTP Microfluidics Shortcourse Copyright 2005 by Steve Wereley, Purdue University

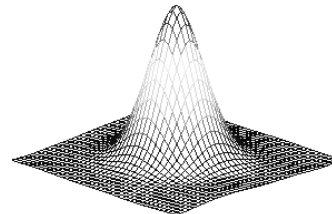
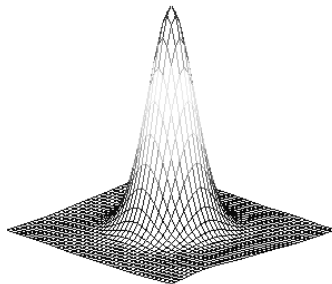


Micro-Particle Image Velocimetry and Thermometry

Hohreiter et al., Meas. Sci. Technol., 2002; Wereley and Hohreiter, Proc. Lisbon conf., 2002

- Based on Brownian motion of tracers broadening correlation peak
- Einstein (1905) developed formula for diffusion coefficient

$$\langle s^2 \rangle = 2D\Delta t \quad \text{where} \quad D = \frac{kT}{3\pi\mu d_p} \quad \Rightarrow \quad \langle s^2 \rangle = \frac{2\Delta t k}{3\pi d_p} \frac{T}{\mu(T)}$$



ICTP Microfluidics Shortcourse Copyright 2005 by Steve Wereley, Purdue University



Particle Imaging Fundamentals

Adrian and Yao, 1983; Olsen and Adrian, 2000

Calculate the particle image size d_e in the object plane:

For light sheet PIV:

$$d_e = \sqrt{M^2 d_p^2 + d_s^2}$$

where M is magnification, d_p is particle diameter, and d_s is spot size of imaging system

For volume illumination (micro-PIV):

$$d_e = \sqrt{M^2 d_p^2 + d_s^2 + d_z^2} \quad d_z = \frac{zMD_a}{(x_0 + z)}$$

ICTP Microfluidics Shortcourse Copyright 2005 by Steve Wereley, Purdue University



Relating Temperature to Peak Area Change

Olsen and Adrian 2000

$$\Delta s_0 = \frac{\sqrt{2}}{\beta} \sqrt{d_e^2 + 8M^2 \beta^2 D \Delta t}$$

where $\beta^2 = 3.67$ is fit parameter for matching Gaussian to Airy function

$$\Delta A = \frac{\pi}{4} (\Delta s_{0,c}^2 - \Delta s_{0,a}^2) = 2\pi M^2 \beta^2 D \Delta t$$

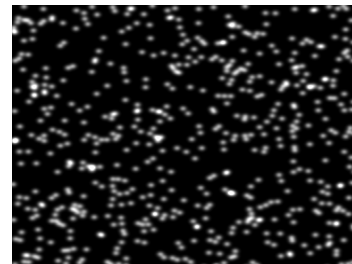
$$\frac{T}{\mu(T)} = \Delta A \frac{3d_p}{2M^2 k \Delta t} = C_0 \frac{\Delta A}{\Delta t}$$



Simulations and Experiments

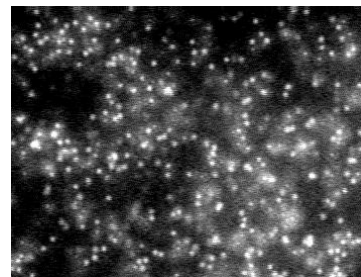
Simulations:

- Matched number density and intensity of experimental images
- No background noise, Gaussian particles
- Effectively laser sheet illumination



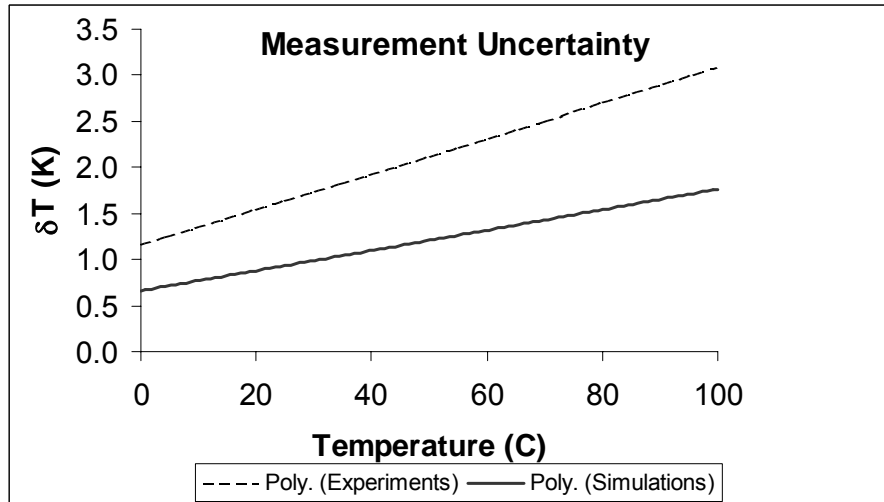
Experiments

- Stagnant particle pool heat with patch heater
- Temperature monitored with thermocouple
- 700 nm PSL particles in DI water
- Volume illuminated microscopic PIV image



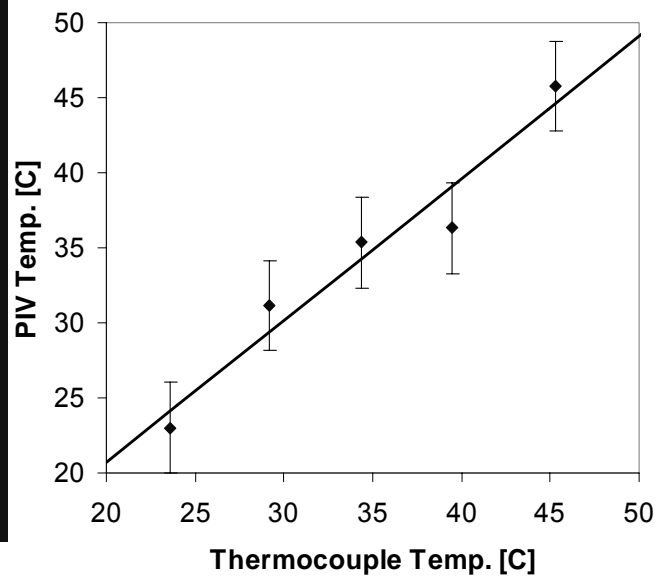
Uncertainty

$$\delta T = \pm T \cdot \left[1 - \frac{T}{\mu} \frac{d\mu}{dT} \right]^{-1} \cdot \sqrt{\left(\frac{\delta(\Delta A)}{\Delta A} \right)^2 + \left(2 \frac{\delta M}{M} \right)^2 + \left(\frac{\delta(\Delta t)}{\Delta t} \right)^2 + \left(\frac{\delta d_p}{d_p} \right)^2}$$

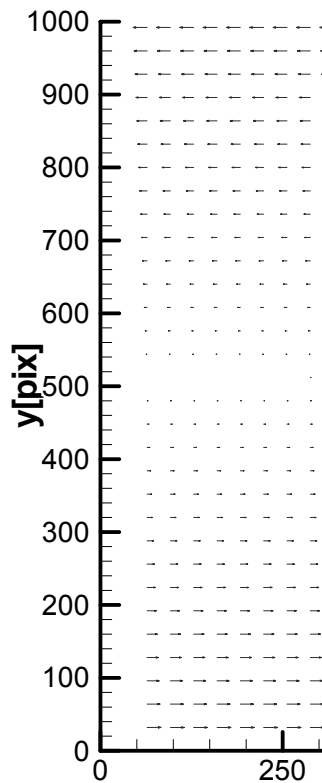


Temperature Measurement Results

- Measure correlation peak areas at e^{-1} level
- Use calibration to get constant of proportionality
- Experiments within $\pm 3^\circ \text{C}$ over significant range
- Simulation accuracy better than $\pm 1^\circ \text{C}$ over larger range



Simultaneous Temperature and Velocity

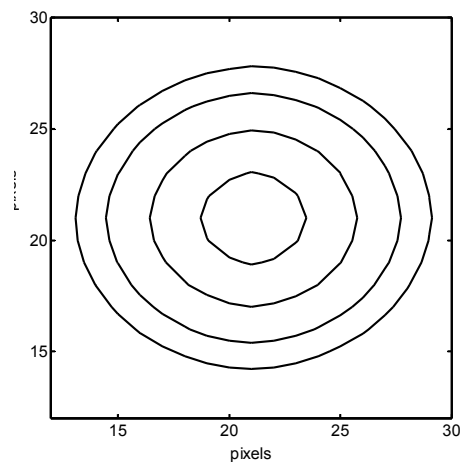
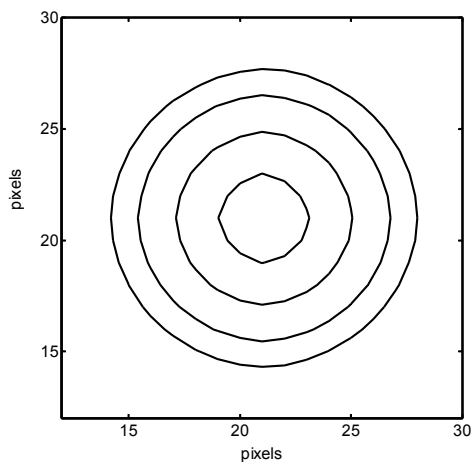


- Perform simulations to assess the viability of this technique
- Need quantifiable shear in the velocity field
 - Simplest flow is 1-D planar shear
 - Used values of 0, 25, 50 pixels displacement gradient over 500 pixels

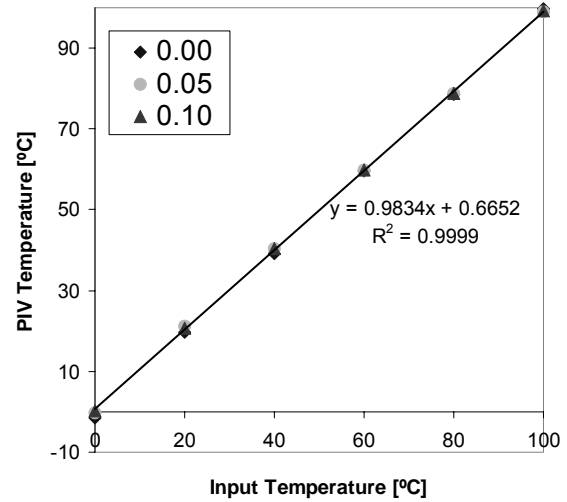
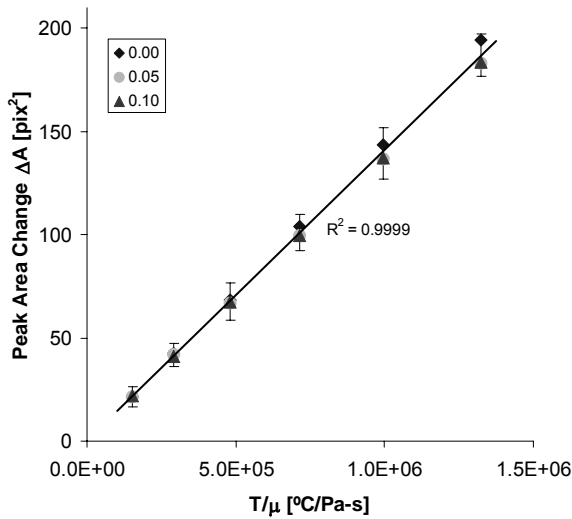


Simultaneous Temperature and Velocity

- In moving fluids, presence of velocity gradients changes peak shapes
- Autocorrelation Cross-correlation



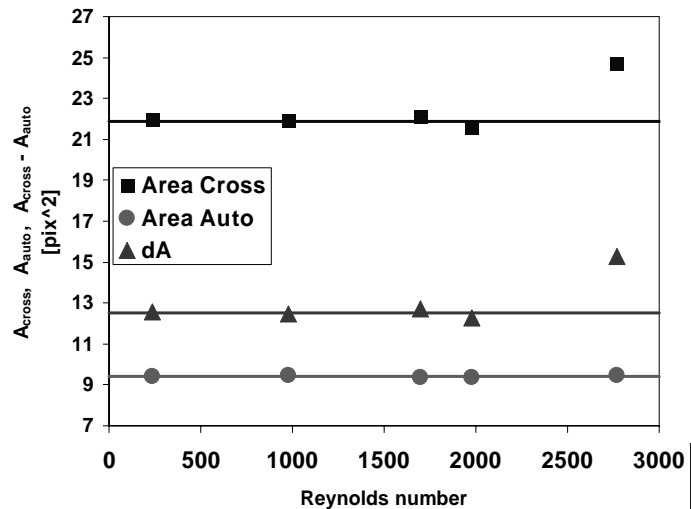
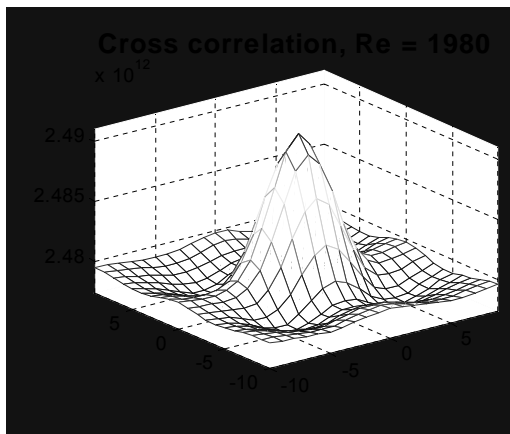
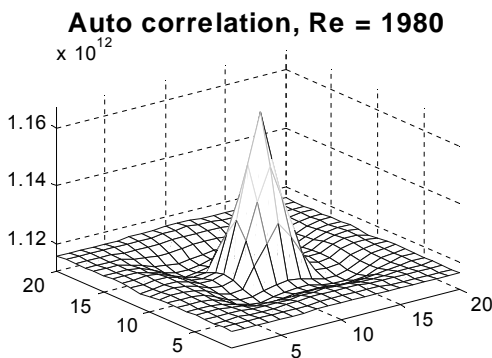
Results in Presence of Flow



- In presence of shear flow, $\pm 0.82^{\circ}\text{C}$ accuracy
- Requires absence of other sources of peak broadening to work



Peak Broadening in Turbulence Transition



Temperature Measurement Summary

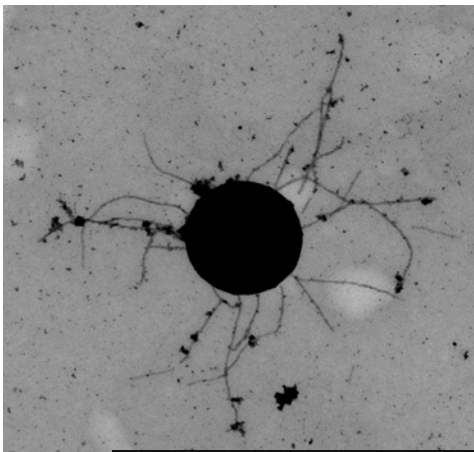
- Can measure fluid temperature using only normal seed particles already in flow
 - spatially-resolved view of temperature field
 - major assumption—only source of peak broadening due to Brownian motion!
- Accuracies on the order of $\pm 1^\circ \text{C}$ even in the presence of velocity field
- Moderate levels of Brownian motion can be averaged away and don't affect velocity accuracy

Assess diffusion coefficient of particle

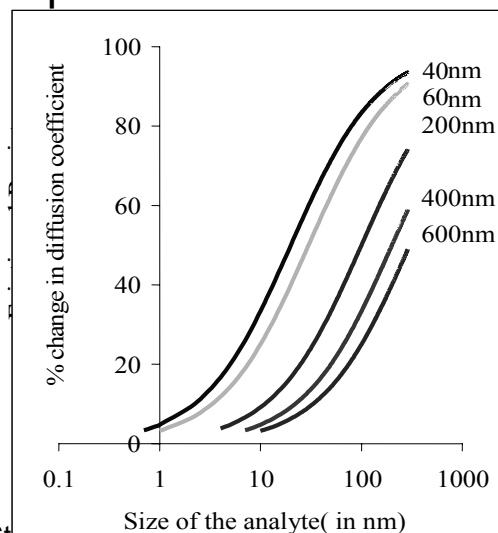
Gorti, Lee and Wereley, "Virus Identification with Particle Image Diffusometry,"

Analytical Chem., 2005 *submitted*

- Use as biodetector for any number of analytes
- Linear behavior for small number of analytes/particle
- Sensitivity of about 1 virus per particle



700 nm particle with 10
M13 viruses attached



Measuring Surface Topology with μ PIV



Measuring Surface Topology with μ PIV

- Another way: Information about surface features contained in velocity profile
- Accurate velocity measurements should allow measurement of surface features
- Solve the inverse problem; i.e. when given the velocity field, find the locations of the boundaries



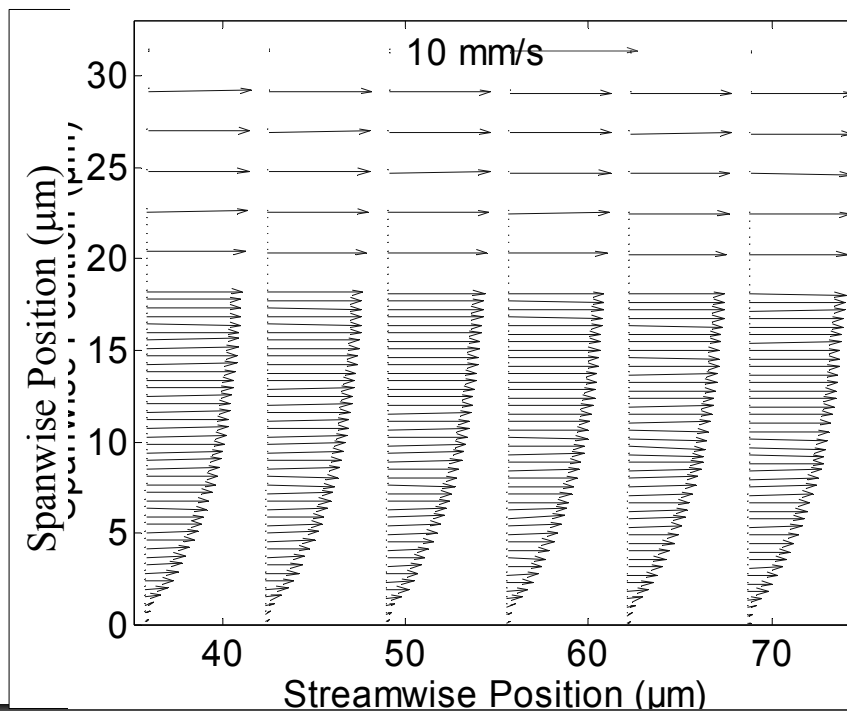
Experiments

- Use flow in rectangular cross section glass capillary to demonstrate concept
- Profilometer used to find glass surface roughness of 2.5 nm
 - essentially smooth wall
- Glass-fluid boundary *calculated* using velocity profile
 - calculated roughness 57 nm

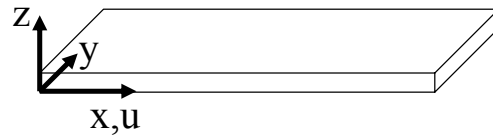


Microchannel Flow (x-z plane)

$y=7\mu\text{m}$ from bottom of channel



Solution for Flow in Rectangular Capillary

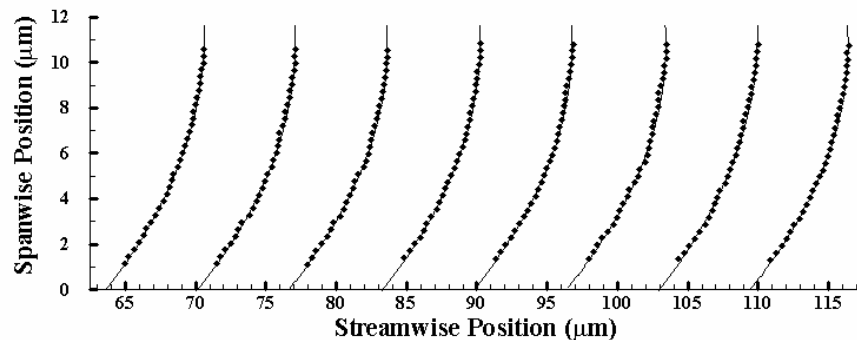
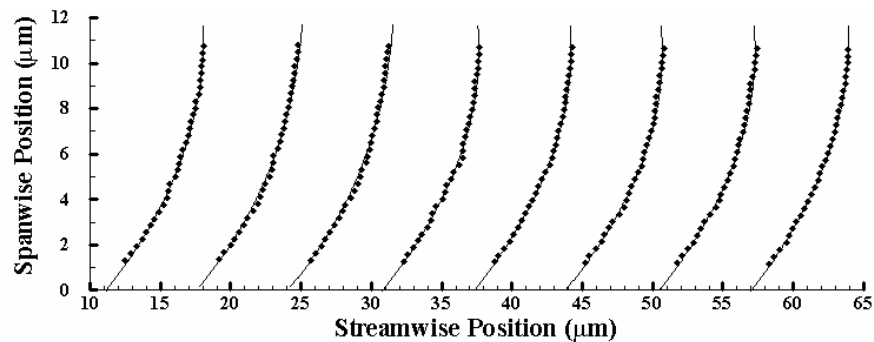


- Given that $-a \leq y \leq a$ and $-b \leq z \leq b$, the velocity in the x direction $u(y,z)$ is:

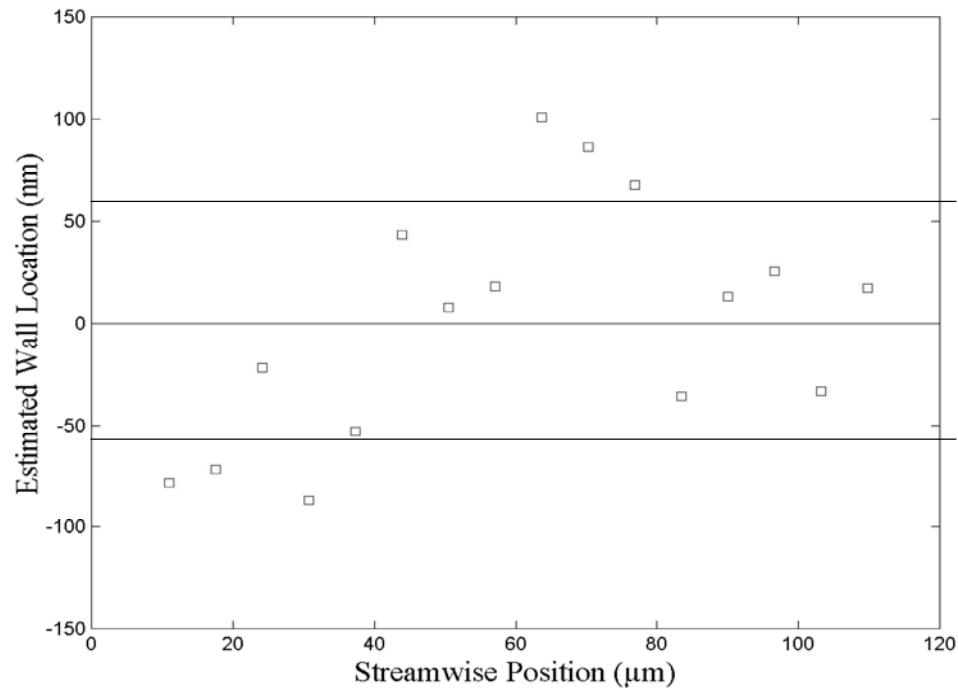
$$u(y,z) = \frac{16a^2}{\mu\pi^3} \left(-\frac{dp}{dx} \right) \sum_{i=1,3,5,\dots}^{\infty} (-1)^{(i-1)/2} \left[1 - \frac{\cosh(i\pi z/2a)}{\cosh(i\pi b/2a)} \right] \times \frac{\cos(i\pi y/2a)}{i^3}$$



Experimental Wall Measurements



Experimental Wall Measurements



Microfluidic References

- **Gad-el-Hak**, "The Fluid Mechanics of Microdevices—The Freeman Scholar Lecture," *J. Fluids Eng.*, Vol. 121, 1999.
- **Gravesen, Branebjerg, and Sondergard**, "Microfluidics--a review," *J. Micromechanics and Microengineering*, Vol. 3, 1993.
- **Ho and Tai**, "Micro-electromechanical systems (MEMS) and Fluid Flows," *Annu. Rev. Fluid Mech.*, Vol. 30, 1998.
- **Karniadakis and Beskok**, *Microflows: Fundamentals and Simulation*, Springer, 2001.
- **Nguyen and Wereley**, *Fundamentals and Applications of Microfluidics*, Artech House, Boston, 2002.
- **Wereley, Gui, and Meinhart**, "Advanced Algorithms for Microscale Velocimetry," *AIAA J.*, Vol. 40, No. 6, pp. 1047-1055 (2002).
- **Wereley and Meinhart**, "Micron Resolution Particle Image Velocimetry," *Micromechanical Diagnostics* Kenny Breuer, ed., (2003) *in press*.